Influence of Resin Composition on the Performance of Composites Reinforced with Recovered Paper and Poultry Feathers

Cosmin Mihai Mirițoiu [a,*] Adrian Sorin Roșca [b] and Adriana Stăncuț [a,*]

The influence of hybrid matrix composition was investigated relative to the mechanical properties of composite materials reinforced with poultry feathers and recovered paper. The matrix composition was modified by varying the proportion of natural dammar resin. The reinforcement remained the same across all formulations and was maintained at a constant 60% by weight in the composite, regardless of the matrix type. The materials were tested under tensile, compressive, and flexural loading, as well as for Shore D hardness and mechanical vibration behavior. It was found that increasing the dammar content enhanced the ductility of the material while reducing its fracture strength, regardless of the destructive testing method applied. In terms of hardness, a decrease was observed with higher dammar content. Additionally, in vibration analysis, an increase in the damping factor and a decrease in the natural frequency were noted as the dammar proportion increased. All these findings were statistically validated using a one-way ANOVA test.

DOI: 10.15376/biores.21.1.808-838

Keywords: Poultry feathers; Dammar resin; Hybrid resin; Mechanical properties; Statistics

Contact information: a: University of Craiova, Faculty of Mechanics, Department of Applied Mechanics and Civil Constructions, Craiova, Romania; b: University of Craiova, Faculty of Mechanics, Department of Vehicles, Transports and Industrial Engineering, Craiova, Romania;
** Corresponding authors: miritoiucosmin@yahoo.com, adriana.stancut@edu.ucv.ro*

INTRODUCTION

Biomass, originating from agricultural and forestry sources as well as biodegradable waste, is used for heat, electricity, and alternative fuels. Its increasing use in the EU supports energy diversification, economic growth, job creation, and a reduction in greenhouse gas emissions. In 2021, bioenergy accounted for about 59% of total renewable energy consumption (European Commission 2023).

Since dammar resin was the variable component in the present hybrid formulations, its main characteristics are briefly outlined. Dammar, obtained from Dipterocarpaceae trees native to Southeast Asia, has been studied for decades (Abdel-Ghani *et al.* 2009; Mittal *et al.* 2010). It is used in paper production, wood finishing, and as a pigment medium (Bonaduce *et al.* 2013; La Nasa *et al.* 2014). Chemically, dammar consists mainly of polycaninene, β-resene, α-resene, and smaller amounts of C15 sesquiterpenes, dammarane units, and pentacyclic triterpenoids (Topp and Pepper 1949; Clearfield 2000; Mittal *et al.* 2010; Mirițoiu 2024). Its incorporation into hybrid matrices has been investigated in terms of both structure and mechanical response (Stănescu 2015; Mirițoiu *et al.* 2020; Franz *et al.* 2021; Ciucă *et al.* 2022), showing that higher dammar content generally reduces composite strength.

As reinforcement, lamellae made of poultry feathers and recovered paper were used. Poultry feathers are mainly keratin-based, typically containing about 91% keratin, 1% lipids, and 8% water (Tesfaye *et al.* 2017; Škerget *et al.* 2023). Their keratin consists largely of amino acids such as serine, glutamate, glycine, leucine, proline, alanine, and valine (Rajabi *et al.* 2020). Reported compositions vary, with some studies indicating ~77% protein, ~7% fat, and ~5% moisture (Tesfaye *et al.* 2017), depending on the isolation or pre-treatment method.

Poultry feathers, by-products of meat production, are often incinerated, releasing pollutants, odors, and toxic leachates harmful to ecosystems (Ossai *et al.* 2022). They are also processed into animal feed *via* hydrolysis, dehydration, and milling, but high costs and low protein quality limit adoption in livestock farming, especially pigs (Park *et al.* 2000). Another approach is soil burial as fertilizer, later abandoned due to groundwater contamination risks (Veerabadran *et al.* 2012).

Poultry feathers are also a source of keratin for cosmetic and pharmaceutical uses, such as shampoos, conditioners, and lotions, due to their skin and hair biocompatibility (Maurya and Singh 2023). Extracted keratin—typically obtained by alkaline digestion, enzymatic hydrolysis, and dialysis— shows benefits in topical products, reducing transepidermal water loss by approximately 30% and increasing skin hydration by up to 22% (Mokrejš *et al.* 2017). Enzymatic keratin hydrolysates are environmentally friendly bioproducts (Brandelli 2008) that have been further applied in hair care, improving hydration, shine, and texture (Villa *et al.* 2013).

Chicken feathers are also applied in construction as thermal and acoustic insulators. Non-woven feather fiber panels show thermal conductivity as low as 0.033 W/(m·K) at 59 kg/m³, which is comparable to wool, recycled PET, and hemp (Dieckmann *et al.* 2021). Epoxy–feather composites achieve thermal resistance up to 0.175 m²K/W at an 80:20 fiber-to-resin ratio, while also providing sound attenuation of 5.5 to 6.7 dB at 500 Hz (Bessa *et al.* 2017). Similarly, treated feather panels can reach conductivity values of 0.0313 to 0.04465 W/(m·K), offering biodegradable, eco-friendly alternatives to conventional insulation (Mrajji *et al.* 2021).

Keratin from poultry feathers emerges as a renewable feedstock for bioplastics and biodegradable films (Gunawan *et al.* 2024). Glycerol-plasticized keratin films show promising mechanical and thermal behavior for packaging (Ramakrishnan *et al.* 2018), while keratin–ginger starch composites achieve high biodegradability (>50% in 12 days) (Oluba *et al.* 2021). Incorporation of microcrystalline cellulose enhances strength and thermal stability, extending applications to food and biomedical fields (Alashwal *et al.* 2020). Recent advances include flexible keratin-based bioplastics (Trojanowska 2023) and the UNLOCK Project (2025), which demonstrates the industrial feasibility of compostable feather-based packaging with improved barrier properties compliant with EU standards.

Poultry feather keratin is widely investigated as a low-cost adsorbent for wastewater treatment. Acid-activated feathers improve dye removal efficiency, following the Langmuir isotherm and pseudo-first-order kinetics (Caovilla *et al.* 2025). Native feathers remove Cu^{2+} with capacities up to 11.5 mg/g, while remaining biodegradable through keratinolytic consortia (Solís-Moreno *et al.* 2021). Keratin modified with graphene oxide or nanochitosan achieves up to 99% removal of multiple heavy metals (Zubair *et al.* 2022). Reviews confirm keratin-derived biopolymers as effective for metal-contaminated effluents (Zahara *et al.* 2021), and studies also highlight their potential in crude oil adsorption (Okoya *et al.* 2020).

Recent work has expanded poultry feather applications to advanced energy and

composite materials. Keratin can be converted into amyloid fibrils yields proton-conductive membranes with 6.3 mS cm^{-1} conductivity and 25 mW cm^{-2} power density, offering biodegradable, low-cost options for fuel cells and electrolysis (Soon *et al.* 2023). Feather fibers are also used as reinforcements, improving dielectric properties in unsaturated polyester composites (Kiew *et al.* 2013), enhancing modulus and yield stress in polyethylene and polypropylene (Barone and Schmidt 2005; Amieva *et al.* 2015), and delivering environmental benefits in PP composites compared with glass fibers (Álvarez-del-Castillo *et al.* 2022). PLA–feather composites show higher mechanical and thermal stability (Cheng *et al.* 2009), while carbonized feather fibers are proposed as lightweight, low-cost hydrogen storage media (Science Daily 2009).

In the last few years, several studies have further consolidated the potential of chicken feather–based composites. Taghiyari *et al.* (2020) show that incorporating chicken feathers into wood–polymeric panels can improve thermal behaviour while maintaining acceptable mechanical performance, indicating their suitability for engineering composite panels. Kurien *et al.* (2022) report that chicken feather fiber reinforced composites can reach competitive tensile and flexural strengths for sustainable structural applications. More recent work focuses on bio-based matrices: Chandran *et al.* (2024) develop bioepoxy composites filled with waste chicken feather fractions, obtaining materials with tailored mechanical and water absorption behaviour. A comprehensive review by Dutta *et al.* (2024) concludes that waste chicken feathers are a versatile filler for a wide range of thermoplastic, thermoset, and biopolymer matrices. As reported in the journal *BioResources*, Paramasivam *et al.* (2025) investigate the mechanical and thermal behaviour of hybrid composites containing chicken feather fibers.

Recovered paper represents the third component in the studied composites. Its main industrial uses include corrugated cardboard and structural packaging, which are valued for low cost and recyclability. Cellulosic fibers derived from waste paper show effective thermal insulation and favorable LCA outcomes (Wang and Wang 2023; Hurtado *et al.* 2016). Shredded office paper is applied in fiberboards, where 50 to 75% recycled content with reduced urea–formaldehyde achieves MOR, MOE, and bond strengths comparable to conventional products (Engin and Konukçu 2024). Recent studies explore cellulose-based insulation combined with animal waste (Petcu *et al.* 2023) or rice husk (Marín-Calvo *et al.* 2023), obtaining thermal conductivity near 0.04 W/m·K and compressive strengths of 20 to 21 MPa. Overall, cellulose insulation from recycled paper is an eco-friendly, efficient material, though wider adoption is still limited by user awareness (Hurtado *et al.* 2016).

Recovered paper is explored in diverse structural and functional applications. Fiberboards containing 50 to 75% shredded office paper and 10 to 15% urea–formaldehyde achieve MOR, MOE, and bond strengths comparable to conventional boards (Engin and Konukçu 2024). Cellulose fiber insulation from recycled paper provides effective thermal and acoustic performance with low embodied energy, though its adoption remains limited (Hurtado *et al.* 2016). Advanced insulation materials, including cellulosic blends with animal waste or rice husk, reach conductivities near 0.04 W/m·K and compressive strengths of 20 to 21 MPa (Marín-Calvo *et al.* 2023; Petcu *et al.* 2023). Recycled paper is also integrated into polymer composites, where structural paper–polypropylene laminates (Prambauer *et al.* 2015), old paper fiber (Zhang and Wang 2012), and recycled office waste (Cioffi *et al.* 2022) improve tensile, flexural, and thermal properties. In cementitious materials, small additions of paper fibers reduce density and conductivity while enhancing flexural strength, toughness, and crack resistance (Stevulova and Čekon 2016; Wang *et al.* 2018; Solahuddin and Yahaya 2022). Beyond construction, paper-based fibers show

potential in filtration: silver nanoparticle-decorated hybrid filters for water purification (Ghodake *et al.* 2020), cellulose nanofiber foams for aerosol capture (Ukkola *et al.* 2021), and phenol–formaldehyde-treated filter paper for oil filtration (Puri and Jatkar 1974).

Despite the increasing number of studies on composites reinforced with natural fibers, chicken feathers, or recycled paper, a significant gap remains regarding systems that simultaneously hybridize both the matrix and the reinforcement using renewable or waste-derived components. The present work addresses this gap by developing and testing hybrid composites consisting of a dammar–epoxy matrix combined with poultry feathers and recovered paper at a fixed total reinforcement level. This dual hybridization concept enables the isolated assessment of the matrix composition effect while maintaining a high bio-based fraction. The novelty of the study lies in demonstrating that such a hybrid configuration can achieve a favorable balance between stiffness, damping, and sustainability, validated through a comprehensive statistical analysis.

In this study, poultry feathers and recovered paper were used as constant reinforcements (60 wt.%), while the matrix (40 wt.%) was varied in dammar resin content (0–70%). Six matrix types were prepared: pure epoxy (100%) and five hybrids with increasing dammar proportions (50%, 55%, 60%, 65%, 70%). The influence of dammar on mechanical performance was examined through tensile, compression, bending, Shore D hardness, and free vibration tests (damping factor and natural frequency). For each material type, two plates (420 × 297 mm) were fabricated, from which 15 specimens were cut; shorter plates (210 × 297 mm) were prepared for compression to prevent buckling. Statistical analysis includes power testing, outlier detection, one-way ANOVA, and validation of assumptions regarding normality and variance homogeneity, ensuring robust interpretation of results.

EXPERIMENTAL

Materials

The composite materials studied in this research consisted of the same reinforcement and six types of matrices: one made of 100% synthetic epoxy resin and five hybrid matrices, where "hybrid" referred to a combination of natural dammar resin (ranging from 50% to 70%) and the remaining portion being synthetic epoxy resin (from 50% down to 30%). The matrices represented the variable component in the fabrication of the composite materials. The component kept constant throughout the study was the reinforcement, consisting of recovered paper strips and poultry feathers. The reinforcement was maintained at a constant mass fraction of 60%, regardless of the type of matrix used. The purpose of varying the matrices was to investigate how their composition influenced the mechanical properties of the resulting composite materials. Dammar resin was sourced from a local supplier (Foita de Aur 2020), while the synthetic epoxy resin was obtained from another local distributor (Polydis 2023). Tables 1 and 2 present the main characteristics of the raw materials used in this study. The synthetic component of the hybrid resins was incorporated in the proportions recommended by the manufacturer. The dammar resin was prepared for use by dissolving it in turpentine, followed by storage in airtight containers.

According to data reported in the literature, pure dammar resin has a high viscosity of approximately 38,000 to 42,000 mPa·s at 25 °C, which makes it difficult to handle in composite processing (Kremer Pigmente, 2024). In contrast, the Resoltech epoxy resins

used in this study had much lower viscosities—typically in the range of 190 to 900 mPa·s at 23 °C, depending on the formulation (manufacturer's data, Resoltech, 2025). To achieve a workable fluidity, the dammar was dissolved in turpentine at a 2:1 mass ratio (dammar: turpentine), which reduced its viscosity to values comparable to those of natural honey (≈ 3,000 to 8,000 mPa·s at 23 °C). The resulting dammar–turpentine mixture retained adequate consistency for lamination while ensuring full wetting of the paper and feather reinforcements. The hybrid matrices were then obtained by combining this bio-based solution with the corresponding epoxy–hardener systems (Resoltech series), mixed in stoichiometric ratios recommended by the manufacturer. All components were homogenized at room temperature (20 to 23 °C). The curing process followed the characteristic behavior of epoxy systems, with a gradual viscosity increase leading to gelation after approximately 25 to 35 minutes, depending on the epoxy formulation. It is important to note that the main purpose of this work was to evaluate the influence of dammar resin content on the mechanical strength and stiffness properties of the composites. Therefore, the viscosity-related assessments were considered qualitative and indicative, serving to describe processability rather than to provide a full rheological characterization.

Table 1. Matrices Utilized in the Fabrication of Composite Materials

Criteria Number	Mass Percentage of the Epoxy Resin Resoltech 1050 (%)	Mass Percentage of the Dammar Resin (%)	Abbreviation
1	100	0	D0
2	50	50	D50
3	45	55	D55
4	40	60	D60
5	35	65	D65
6	30	70	D70

Table 2. Main Characteristics of the Raw Materials Used in the Study

Raw Material	Type and Origin	Main Components	Density (g/cm^3)	Key Properties	References
Poultry Feathers	Waste from Romanian poultry farms	Keratin, lipids and moisture	0.002 to 0.005	Lightweight, flexible, low thermal conductivity, biodegradable	Tesfaye *et al.* (2017); Škerget *et al.* (2023)
Recovered paper	Office paper	Cellulose fibers, fillers, starch	0.70 to 0.80	Recyclable, good fiber–resin adhesion, structural stability	Engin and Konukçu (2024)
Dammar resin	Natural exudate from Dipterocarpaceae trees	Polycaninene, β-resene, triterpenoids	1.04 to 1.10	Natural resin, enhances ductility in hybrid matrices	Franz *et al.* (2021); Miriţoiu *et al.* (2020)
Epoxy resin	Synthetic epoxy resin	Bisphenol-A epoxy + hardener	1.10 to 1.15	High strength, stiffness, good adhesion, low shrinkage	Polydis (2023); Resoltech (2025)

The values summarized in Table 1 (up to 70 wt% natural dammar resin) were selected based on previous findings indicating that, when this threshold was surpassed, the composite matrix exhibited a pronounced reduction in mechanical performance—approximately 3.5-fold in tensile strength and nearly sixfold in elastic modulus—relative to systems without dammar resin (for instance, Franz *et al.* 2021). Furthermore, a dammar content lower than 50 wt% was not selected, as the aim was to employ hybrid matrices with a high proportion of natural dammar, starting from a minimum threshold of 50 wt% dammar and 50 wt% synthetic resin.

Comprehensive FTIR, TGA, and Raman analyses of hybrid dammar–epoxy resins with compositions equivalent to those employed in this work had been extensively reported in the authors' previous publications (Mirițoiu *et al.* 2020; Bolcu *et al.* 2024). According to Mirițoiu *et al.* (2020), the thermogravimetric analysis identified five stages of thermal degradation. The initial mass loss occurred at approximately 94 to 100 °C, corresponding to moisture evaporation. A major decomposition process followed between 245 and 365 °C, associated with the degradation of the dammar and epoxy resin components. The material underwent complete decomposition up to about 800 °C, leaving no significant residual mass beyond this temperature. According to Bolcu *et al.* (2024), the FTIR and Raman analyses revealed that the intensity of the characteristic absorbance bands decreased progressively as the proportion of dammar resin increased. In addition, the overall quality and sharpness of the Raman spectra diminished at higher dammar contents, suggesting that the chemical composition and hybridization degree significantly affected the final structure of the matrix.

As this study involves statistical analyses to evaluate the effect of resin composition on mechanical performance, the composites containing a matrix entirely of synthetic resin and reinforced with poultry feathers and recovered paper served as the reference samples.

Methods

In producing the composite materials, the reinforcement consisted of a blend of recovered paper and poultry feathers. The recovered paper served as a structural support for the proper alignment of poultry feathers during the lamina fabrication process. Preliminary tests performed without the paper base showed that laminae made only of feathers and resin were prone to deterioration and loss of shape during demolding. Therefore, recovered paper was introduced to provide dimensional stability, to facilitate handling during stacking, and to ensure the formation of continuous, rigid composite plates after polymerization. Its cellulosic composition also favored resin penetration and adhesion between layers. The hand lay-up method was employed, applying the layers sequentially. First, a thin coat of resin was brushed onto a standard office paper sheet (IQ Economy+, 420 × 297 mm), obtained from a local supplier (see IQ Economy+ 2024). Next, poultry feathers were positioned manually in parallel alignment over the resin-coated surface while the resin remained in its gel stage, ensuring proper wetting and adhesion. The resin application aimed to secure and bond the feathers to the paper surface, forming a reinforced lamina. This procedure was repeated to produce nine laminae, which were subsequently stacked to create a layered composite. A thin resin layer was applied between laminae before stacking, followed by pressing under a uniformly distributed load of 3kN over an area of 420 × 297 mm² (meaning a pressure of approximately 0.024 MPa distributed on the surface area) to achieve consistent thickness and consolidation. The fabrication was performed under laboratory conditions (20 to 23 °C, normal humidity). The feathers were used without chemical pretreatment, being only cleaned and air-dried prior to embedding.

The mass ratio between recovered paper and feathers was maintained at 30 wt.% each, corresponding to a total reinforcement content of 60 wt.% in all formulations. The reinforcement fraction, consisting of 30 wt.% recovered paper and 30 wt.% poultry feathers, was determined by gravimetric control, each component being weighed before lamination to ensure a consistent total reinforcement content of 60 wt.%. A visual inspection confirmed uniform laminate thickness, and the manual alignment process ensured a quasi-unidirectional orientation across each layer.

Fig. 1. a. An example of a lamina made of poultry feathers and recovered paper; b. detail highlighting the poultry feathers and recovered paper

Fig. 2. An example of applying resin to the lamina using hand lay-up

The Resoltech epoxy resin used as the reference material exhibited a curing time of approximately 24 to 48 h under laboratory conditions (20 to 23 °C). In contrast, the hybrid dammar–epoxy formulations required longer curing periods, depending on the dammar content. The D50 composition reached full solidification after about 5 days, D55 after 5–6 days, D60 after 7 days, D65 after 8 days, and D70 after 9 to 10 days. This progressive increase in curing time is attributed to the partial substitution of epoxy resin with natural dammar, which slows down the cross-linking reactions and the diffusion of hardener

components. Although no separate DSC curing analysis was performed, the completion of the curing process was confirmed visually—by the loss of surface tackiness and by verifying that the specimens had fully solidified before testing. This behavior is consistent with other studies on bio-epoxy hybrid systems (see for example Bolcu *et al.* 2024). The applied load was maintained daily until the cutting stage, with the weight removed only on the day of specimen trimming. An example of a lamina during the casting process is shown in Fig. 1a. In Fig. 1b, the two reinforcement-type components that form part of a lamina's structure are highlighted: poultry feathers and recovered paper. An example of applying the resin layer over the laminae is shown in Fig. 2. Another example of one of the plates obtained through the hand lay-up process is presented in Fig. 3.

Fig. 3. An example of one of the D70 final plates obtained by hand lay-up

Test Standards and Characterizations

Tensile test

For the tensile strength investigation, composite plates were fabricated using recovered paper fibers in combination with discarded chicken poultry feathers as reinforcement, along with the four resin formulations listed in Table 1 (one synthetic and three bio-derived alternatives). From each manufactured plate, a total of fifteen test coupons were obtained. The tensile tests were performed according to the ASTM D3039/D3039M-08 (2014) standard, using samples measuring 250 mm in length, 25 mm in width, and 8 mm in thickness. The measurements were carried out with an Instron 1000 HDX (Instron, Norwood, MA, USA) universal testing machine.

Compression test

For the compression strength evaluation, composite plates—similar in construction to those prepared for tensile testing—were produced, but with the specific feature of incorporating 19 stacked laminae. Test specimens were cut to dimensions of roughly 15 mm in length, 15 mm in width, and 15 mm in thickness. The compression tests were conducted in accordance with the ASTM D695-23 (2016) standard. An LGB universal testing system (LGB Testing Equipment, Azzano San Paolo, Italy), fitted with a dedicated compression test fixture, was utilized for the procedure. The choice of 19 layers provided

adequate specimen thickness to encourage failure by compressive crushing rather than premature instability from buckling.

Bending test

For the flexural strength analysis, composite plates analogous to those employed in tensile trials were produced, utilizing recycled paper together with poultry feather fragments as reinforcing elements, embedded within a matrix composed of the eight resin formulations listed in Table 1. The lay-up maintained the same 10-layer arrangement as applied in the tensile investigation. From each manufactured plate, fifteen specimens were accurately cut to dimensions of 200 mm in length, 32 mm in width, and 8 mm in thickness. Testing was performed using an LGB universal testing system (LGB Testing Equipment, Azzano San Paolo, Italy) fitted with a three-point bending fixture. The flexural evaluation followed the ASTM D790-17 (2017) standard.

Vibration test

The specimens employed for the vibration assessment preserved the same dimensions and properties as those outlined in the tensile testing section. Each was rigidly fixed at one end, with the opposite end left free to which a Brüel & Kjær accelerometer (sensitivity: 0.04 pC/ms^2) was mounted. The accelerometer was connected to a Nexus signal conditioning module, which relayed the output to a SPIDER 8 data acquisition system (HBK Hottinger Brüel & Kjær, Darmstadt, Germany). The SPIDER 8 unit was then interfaced with a laptop, where the experimental measurements were logged for further analysis.

Shore D hardness test

The Shore D hardness evaluation was carried out following the ASTM D2240-15 (2017) standard. Test pieces identical in size to those described in the tensile testing section were employed. A total of five readings were recorded along each specimen at 50 mm intervals, with the end points located 25 mm from either edge. All measurements were taken along the central axis of the specimen's width to maintain consistency in the results.

Statistical Interpretation of Experimental Data

This study investigated the influence of dammar resin content on the mechanical properties of the composite materials. The statistical analysis aimed to verify whether the observed differences among the experimental results were significant. The workflow included statistical power testing to confirm sample adequacy, Dixon's test for outlier detection, and one-way ANOVA to evaluate the influence of resin composition. The validity of ANOVA results was checked using Levene's test (homogeneity of variances) and the Shapiro–Wilk test (normality of data distribution). Finally, a post hoc ANOVA with Bonferroni correction was applied to identify significant pairwise differences between groups. All analyses were performed using Microsoft Excel (Microsoft Corp., Redmond, WA, USA).

Statistical power expresses the probability that a test correctly detects a true effect. It was computed according to Mirițoiu (2025) using the sample mean, standard deviation, size (n = 15), standardized value v_s (Eq. 1), effect size (Eq. 2), t-statistic (Eq. 3), and resulting power P (Eq. 4). When P=1, the test fully confirms the adequacy of the sample size.

$$\delta = \bar{x} - v_s \quad (1)$$

$$d = \frac{\delta}{s} \quad (2)$$

$$t = \frac{\bar{x} - v_s}{\frac{s}{\sqrt{n}}} \quad (3)$$

$$P = 1 - \Phi(z_{critic} - \delta) + \Phi(-z_{critic} - \delta) \quad (4)$$

The parameter $z_{critic} = 1{,}96; 1{,}645; 2{,}576$ for α=0,05;0,1;0,01, where α is the significance treshold.

To remove outlier values, the Dixon test was applied. This method is recommended for datasets containing fewer than 25 values. The dataset was arranged in ascending order, and Q was calculated using Eq. 5,

$$Q = \left| \frac{x_j - x_{j+1}}{x_{\max} - x_{\min}} \right| \quad (5)$$

where *j* denotes the potentially aberrant value, $j + 1$ the nearest value, and x_{max} and x_{min} the maximum and minimum of the dataset, respectively. The significance level α (typically 0.05 or 0.01) was used to obtain the critical value Q_{critic} from literature tables (Stanimir and Pascu 2014). Values with $Q > Q_{critic}$ were classified as outliers and removed.

A one-way ANOVA was applied to evaluate whether the dammar resin content significantly affected the mechanical properties. This test determines whether differences among group means are statistically significant. Equal means indicate that dammar percentage has no effect, while unequal means confirm a significant influence (Ott and Longnecker 2021).

According to Zar (1999), in a one-way ANOVA, the overall mean of all observations is calculated using Eq. 6,

$$\bar{X} = \frac{\sum X_{ij}}{N} \quad (6)$$

where X_{ij} represents the individual values and *N* denotes the total number of data points across all groups.

The mean for each group was computed using Eq. 7,

$$\bar{X}_i = \frac{\sum X_i}{n_i} \quad (7)$$

where X_i represents the values in group i, and n_i is the number of observations within that group.

The sum of squares between groups and the sum of squares within groups were calculated using Eqs. 8 and 9, respectively.

$$SS_B = \sum n_i \cdot (\bar{X}_i - \bar{X})^2 \quad (8)$$

$$SS_W = \sum n_i \cdot \left(\sum X_{ij} - \sum X_i\right)^2 \quad (9)$$

The degrees of freedom for the variation between groups and within groups were obtained using Eqs. 10 and 11, where *k* denotes the number of groups and *N* represents the total number of observations.

$$df_B = k - 1 \quad (10)$$

$$df_W = -k + N \quad (11)$$

The mean squares for the variation between groups and within groups were calculated using Eqs. 12 and 13, respectively.

$$MS_B = \frac{\sum n_i \cdot (\overline{X_i} - \bar{X})^2}{k-1} \quad (12)$$

$$MS_W = \frac{\sum n_i \cdot \left(\sum X_{ij} - \sum X_i\right)^2}{-k+N} \quad (13)$$

The F-value was determined by dividing Eq. 12 by Eq. 13 and compared with the critical F-distribution values for the corresponding degrees of freedom. The resulting p-value represents the probability of obtaining an equal or greater F-value under the null hypothesis.

Levene's test was applied to verify the homogeneity of variances, a key assumption of ANOVA. This test checks whether group variances differ significantly; if they do, the ANOVA assumptions may be invalid (Ott and Longnecker 2021; Tărâță *et al.* 2020). The procedure involved grouping the data, computing deviations from each group mean (Eq. 14), forming the z dataset (Eq. 15), and performing ANOVA on these values. The resulting F-value was compared with the critical value from statistical tables (Stanimir and Pascu 2014; Mirițoiu 2025).

$$Z_{ij} = \left| x_{ij} - \bar{x} \right| \quad (14)$$

$$z_{ij} = \left| x_{ij} - y_i \right| \quad (15)$$

The Shapiro–Wilk test was applied to verify the normality of data within each group. This test assesses whether the distribution of values deviates significantly from normality, which may affect the validity of ANOVA (Shapiro and Wilk 1965). The *p-value* was calculated using Eq. 16, where n is the sample size, x_i the data points, a_i the Shapiro–Wilk coefficients, and $\bar{x}$ the sample mean (Statistics Kingdom 2025).

$$p = p_1 + \frac{\frac{\left(\sum_{i=1}^{n} a_i \cdot x_i\right)^2}{\sum_{i=1}^{n} (x_i - \bar{x})^2} - W_1}{W_2 - W_1} \cdot (p_2 - p_1) \quad (16)$$

The parameters W_1, W_2, p_1, and p_2 are available in statistical tables—for example, in Real Statistics (2025).

A post hoc ANOVA with Bonferroni correction was applied to identify significant pairwise differences after ANOVA. The Bonferroni adjustment minimized Type I errors in multiple comparisons (Juarros-Basterretxea et al. 2024). These methods efficiently determined the influence of dammar resin content on mechanical properties (Popescu *et al.* 2023).

When group variances were unequal, the Welch ANOVA procedure was used as an alternative to the standard one-way ANOVA to prevent false-positive results (Delacre et al. 2019). In this approach, the null hypothesis (H_0) assumes equal group means, while the alternative (H_a) states that at least one mean differs. Group means ($\bar{X}_i$) and variances (S_i^2) were calculated using Eqs. 17 and 18, where X_{ij} denotes individual observations and n_i the number of elements per group.

$$\overline{X_i} = \frac{\sum X_{ij}}{n_i} \quad (17)$$

$$S_i^2 = \frac{\sum\left(X_{ij} - \overline{X_i}\right)^2}{n_i - 1} \quad (18)$$

The pooled mean of all groups $\overline{X_W}$ was derived following Eq. 19.

$$\overline{X_W} = \left(\sum \frac{\overline{X_i}}{S_i^2}\right) \cdot \left(\sum S_i^{-2}\right)^{-1} \quad (19)$$

For a number of k groups, the computation of the Welch statistic (F_W) was performed based on Eq. 20.

$$F_W = \frac{\sum^{n_i\left(\overline{X_i} - \overline{X_W}\right)^2}_{S_i^2}}{-1+k} \quad (20)$$

The variance in the denominator term, denoted as D_V, was derived using Eq. 21.

$$D_V = \sum \left(\frac{n_i - 1}{n_i}\right) \cdot S_i^{-4} \quad (21)$$

Equations 22 and 23 are applied to compute the degrees of freedom in the case of unequal variances.

$$df_1 = -1 + k \quad (22)$$

$$df_2 = \frac{\left(\sum \frac{1}{S_i^2}\right)^2}{\sum\left(\frac{n_i - 1}{n_i}\right) \cdot S_i^{-4}} \quad (23)$$

To establish the decision criterion, the critical F-value ($F_{\propto, df_1, df_2}$) was derived from the F-distribution corresponding to the selected significance level (typically 0.05). When the result from Eq. 20 is greater than the critical F-value, the null hypothesis is not retained, demonstrating the existence of meaningful differences among the group means.

RESULTS AND DISCUSSION

Tensile Test

In the tensile evaluation, fifteen samples were obtained from each cast plate produced with the six resin systems presented in Table 1. The specimens were cut according to the poultry feathers' orientation, and the strength test was performed along the direction of reinforcement.

Figure 4 presents the stress–strain curves at fracture for one representative specimen from each of the six tested material types. A single characteristic curve was selected for each material to maintain clarity, as plotting all individual curves in the same figure would have resulted in an overcrowded and difficult-to-interpret graph. The experimental results of the tensile breaking strength and elongation at break for all 15 specimens from each material set are presented in Figs. 5 and 6.

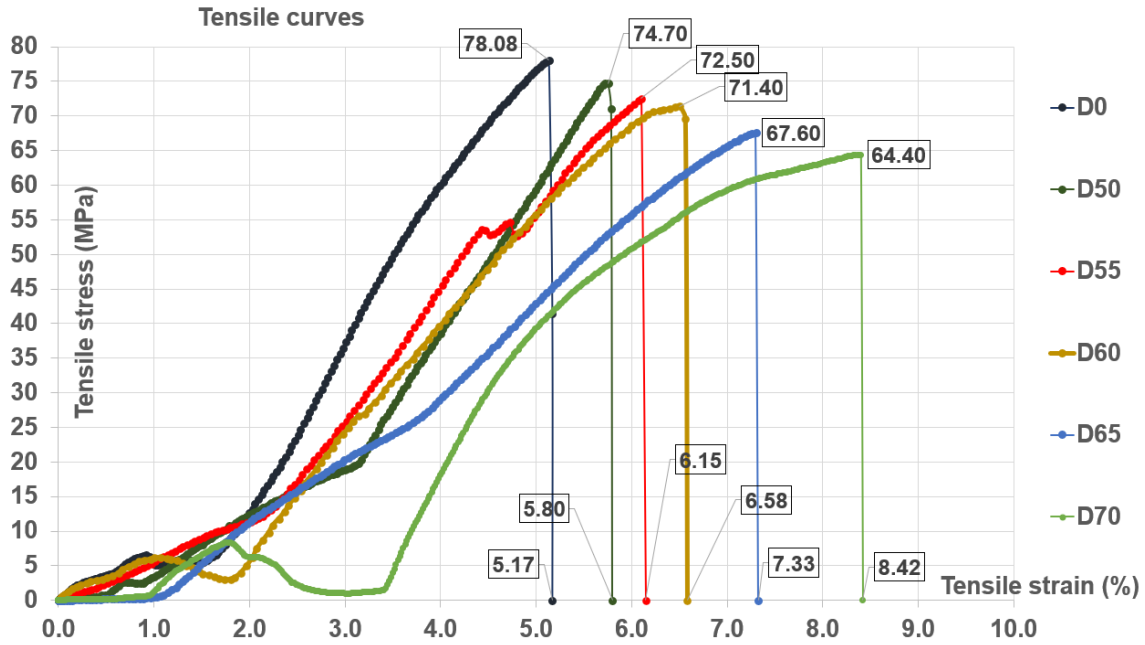

Fig. 4. Characteristic stress–strain curves for one specimen from each of the six material types

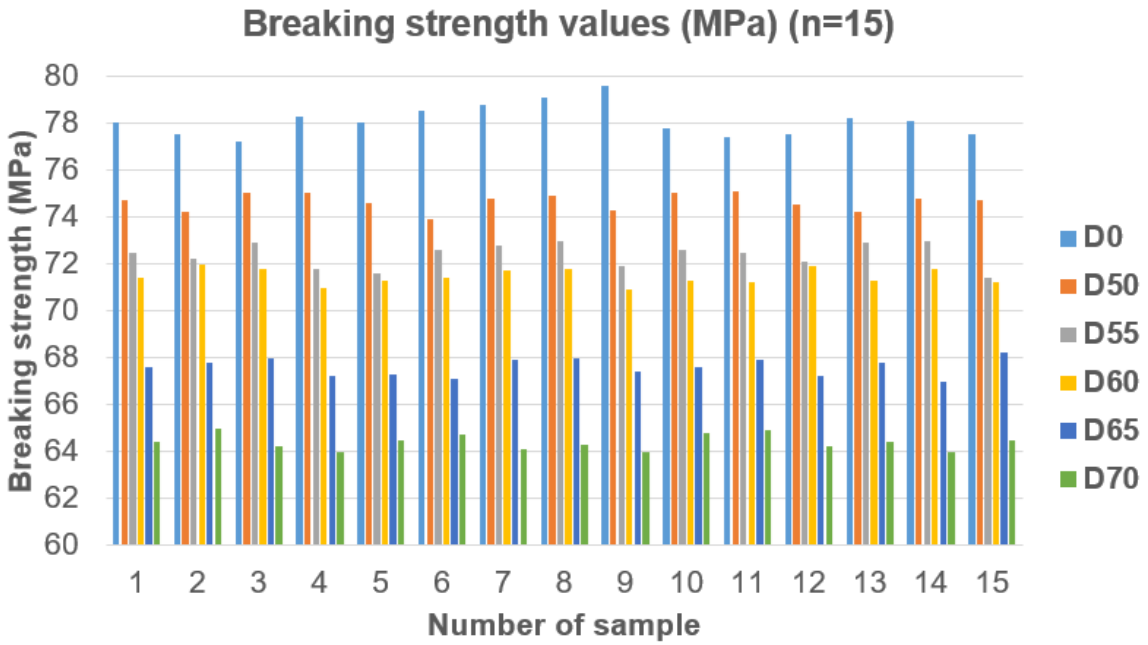

Fig. 5. Tensile breaking strength for the 15 specimens of each material set

The resin composition significantly influenced the tensile properties, as increasing the dammar fraction led to higher ductility (greater elongation at break) but a corresponding reduction in tensile strength. This effect was found to be statistically significant.

A statistical power analysis confirmed that testing 15 specimens per group ensured highly reliable results for both tensile strength and elongation at break (power ≈ 1). No outliers were detected (Dixon test, $\alpha = 0.05$). One-way ANOVA showed that dammar content had a highly significant effect on tensile strength ($F = 1748.9$, $p = 2.6\times10^{-63}$) and elongation at break ($F = 13021.0$, $p = 8.9\times10^{-120}$). Levene's ($p > 0.05$) and Shapiro–Wilk

($p > 0.05$) tests confirmed homogeneous variances and normal distributions. The Bonferroni post-hoc analysis ($\alpha = 0.01$) indicated that all consecutive group pairs showed significant differences ($p < 0.01$), confirming a consistent effect of increasing dammar content on tensile behavior.

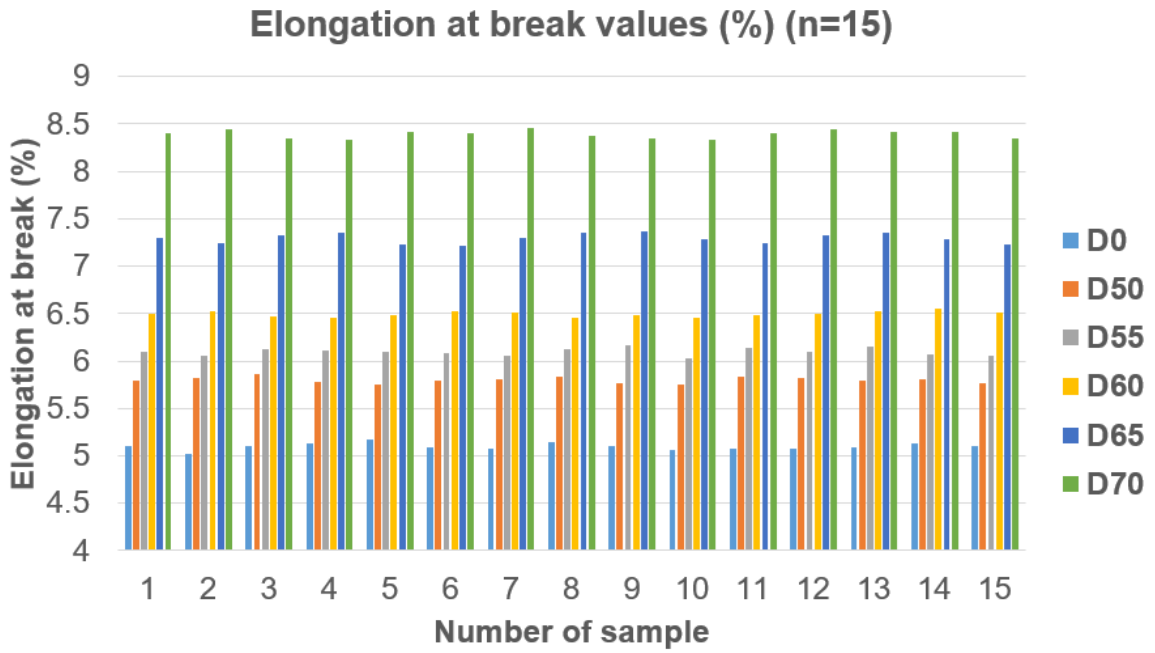

Fig. 6. Elongation at break for the 15 specimens of each material set

Compression Test

In the compression experiment, the methodology mirrored that of the tensile test: fifteen samples were obtained and tested from each material mentioned in Table 1. The results are presented in Figs. 7 and 8.

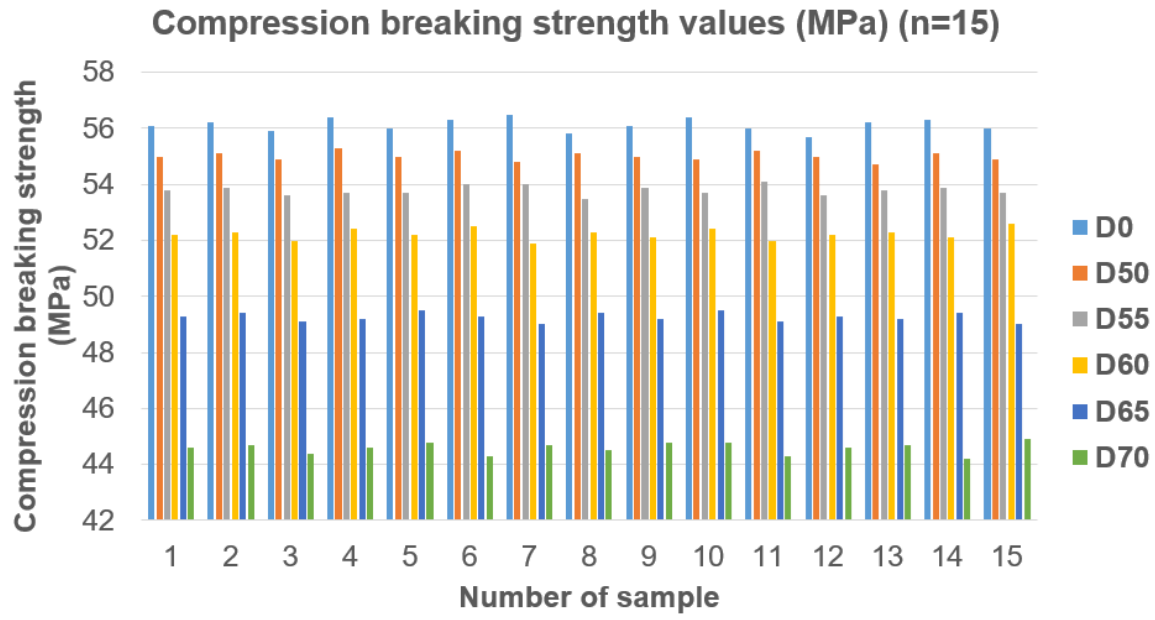

Fig. 7. Compression breaking strength for the 15 specimens of each material set

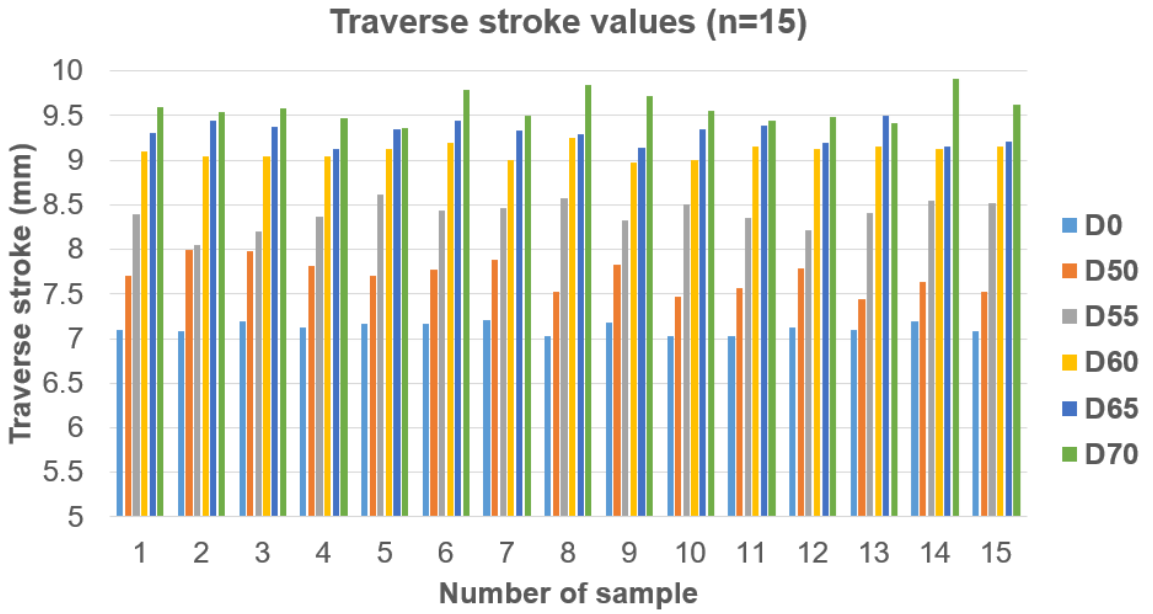

Fig. 8. Traverse stroke for the 15 specimens of each material set (compression test)

The compression test results followed the same trend as the tensile behavior, with higher dammar content leading to increased deformability but reduced compressive strength; these effects of resin composition were further evaluated for statistical significance.

A statistical power analysis confirmed that testing 15 specimens per group provided highly reliable results for both compressive strength and displacement (power ≈ 1). No outliers were identified (Dixon test, $\alpha = 0.05$). One-way ANOVA showed that dammar content had a strong influence on compression strength ($F = 7555.6$, $p = 7.3\times10^{-110}$) and deformation ($F = 802.6$, $p = 2.6\times10^{-69}$).

Levene's test confirmed variance homogeneity for compressive strength ($p = 0.62$), but not for deformation ($p = 0.011$); therefore, Welch ANOVA was applied, confirming a significant effect of dammar percentage ($p = 2.6\times10^{-82}$). Shapiro–Wilk tests verified normal data distribution ($p > 0.05$). The Bonferroni post hoc test ($\alpha = 0.01$) showed significant differences for all consecutive group pairs, confirming that each incremental increase in dammar content produced measurable changes in compressive properties.

Bending Test

During the flexural evaluations, the applied methodology was comparable to the approach used in both tensile and compressive experiments. The results are presented in Figs. 9 and 10.

Similarities were noted with the tensile and compression tests. The bending tests confirmed that higher dammar content reduced strength but increased deformation, reflecting greater ductility of the hybrid matrix; these effects were later verified statistically for significance.

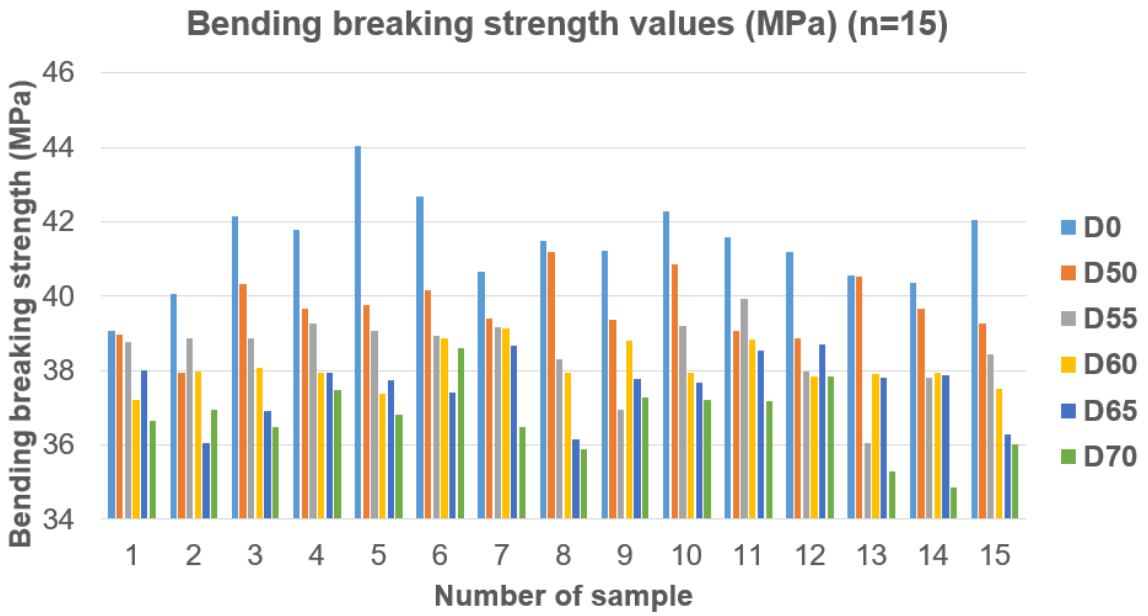

Fig. 9. Bending breaking strength for the 15 specimens of each material set

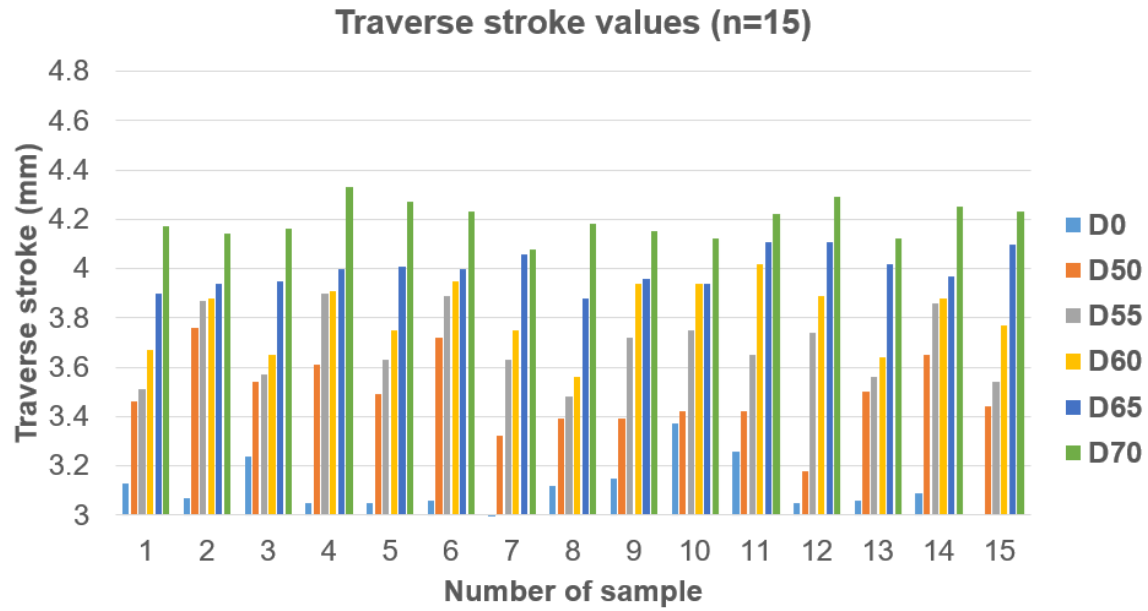

Fig. 10. Traverse stroke for the 15 specimens of each material set (bending test)

A statistical power analysis confirmed that testing 15 specimens per group provided reliable results for both flexural strength and displacement (power ≈ 1). No outliers were found (Dixon test, $\alpha = 0.05$). One-way ANOVA showed a highly significant effect of dammar content on flexural strength ($F = 48.5$, $p = 2.4\times10^{-23}$) and deformation ($F = 153.9$, $p = 9.4\times10^{-41}$). Levene's ($p = 0.43$ and 0.08) and Shapiro–Wilk ($p > 0.05$) tests confirmed homogeneity of variances and normality of data distribution. The Bonferroni post hoc analysis ($\alpha = 0.01$) revealed that only the initial increase in dammar content (0–55%) produced statistically significant reductions in bending strength, while further increases had diminishing effects. Conversely, bending deformation increased significantly with dammar content, indicating enhanced ductility and flexibility of the hybrid matrix.

Vibration Test

For the vibration tests, the specimens were rigidly fixed at one end in a vice mounted on a solid table, ensuring adequate stability throughout the experiment. Each sample was evaluated with a free length of 180 mm. Damping characteristics were determined by the logarithmic decrement method (Mirițoiu 2024). The results are presented in Figs. 11 and 12. The Brüel & Kjær Type 8309 accelerometer (3 g according to BKSV 2025) had a negligible influence on the vibration results, as the specimen mass exceeded 20 g, resulting in a mass ratio <15%. The corresponding shift in natural frequency was estimated to be less than 3%, which is within the experimental uncertainty range.

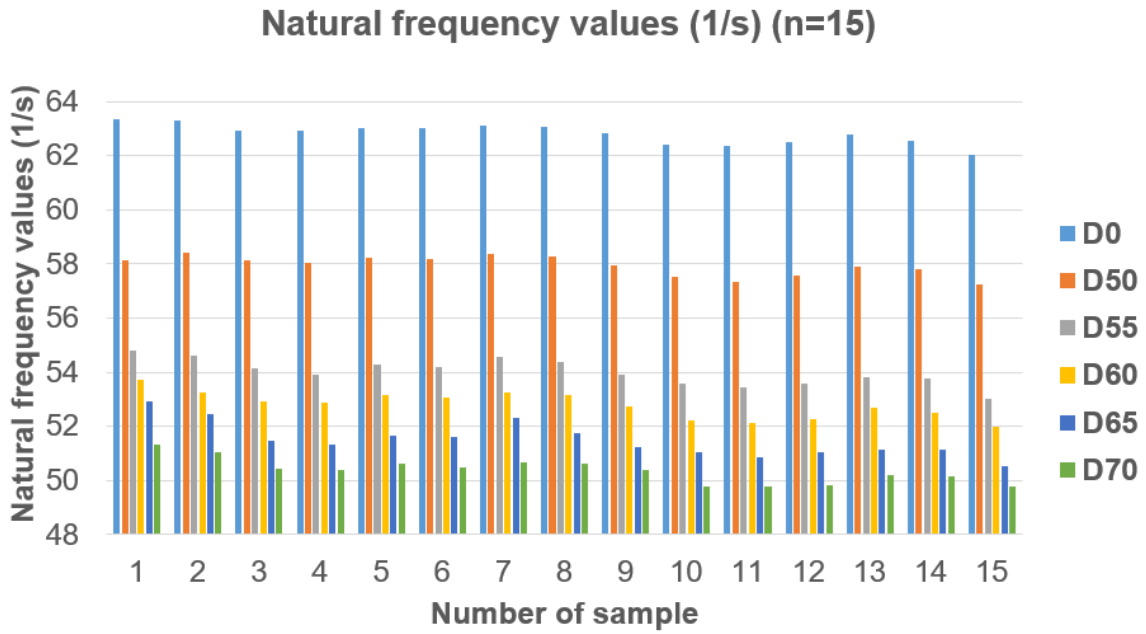

Fig. 11. Natural frequency for the 15 specimens of each material set

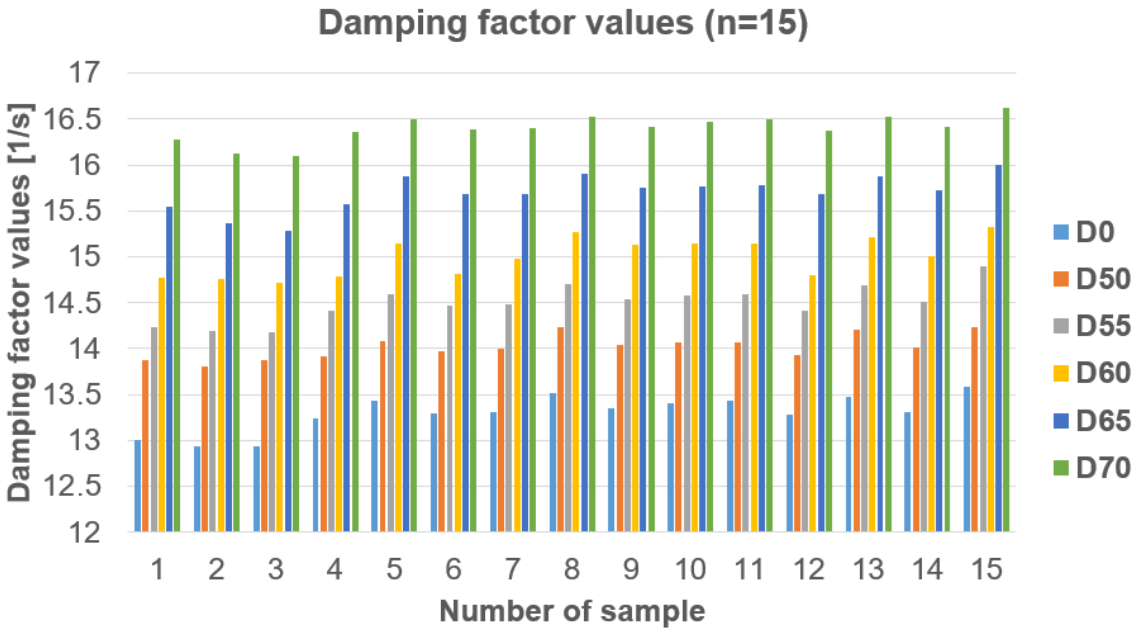

Fig. 12. Damping factor for the 15 specimens of each material set

The vibration analysis confirmed that increasing the dammar content lowered the natural frequency but enhanced the damping factor. This inverse relationship reflects reduced stiffness and greater elasticity of the hybrid matrix, consistent with mechanical tests showing higher deformability and ductility at elevated dammar levels.

A statistical power analysis confirmed that testing 15 specimens per group ensured highly reliable results for both natural frequency and damping factor (power ≈ 1). No outliers were identified (Dixon test, $\alpha = 0.05$). One-way ANOVA revealed that dammar content had a very strong influence on both natural frequency ($F = 1429.8$, $p = 1.1\times10^{-79}$) and damping factor ($F = 578.7$, $p = 1.7\times10^{-63}$). Levene's ($p = 0.52$ and 0.36) and Shapiro–Wilk ($p > 0.05$) tests confirmed homogeneous variances and normally distributed data. Post hoc Bonferroni analysis ($\alpha = 0.01$) showed that all consecutive group pairs exhibited significant differences ($p < 0.01$). The results indicate that increasing dammar content consistently decreases the natural frequency while significantly increasing the damping factor, confirming reduced stiffness and enhanced energy dissipation capacity.

Shore D Hardness Test

The final experimental test consisted of measuring the hardness of the materials on the Shore D scale. Hardness was measured at 15 points along the longitudinal axis of symmetry of the specimen. All data were consolidated in Fig. 13.

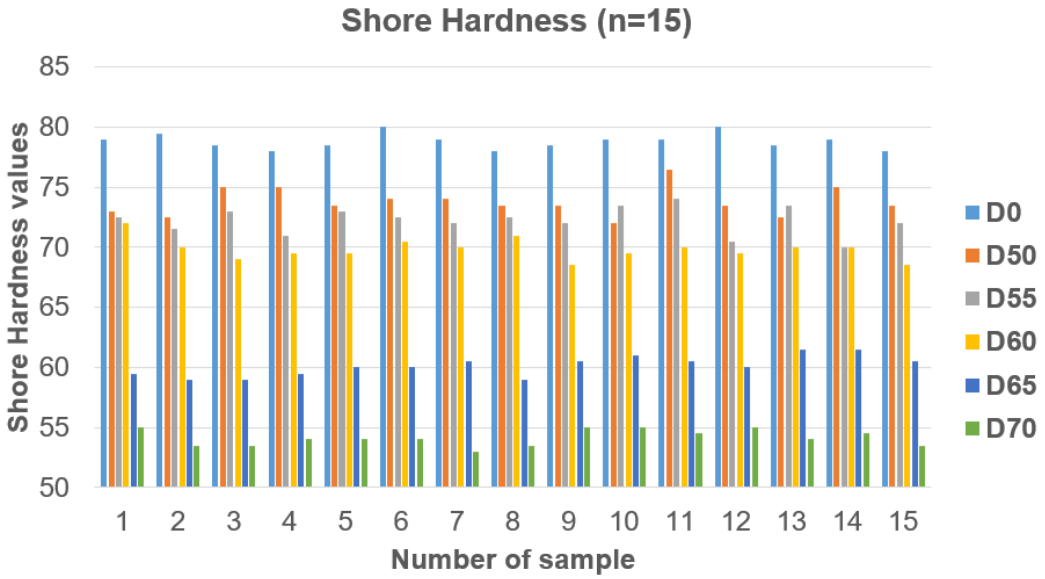

Fig. 13. Shore D hardness for the 15 specimens of each material set

Material stiffness can be described as the capacity of a substance to withstand shape changes when subjected to external forces. A smaller degree of deformation under a constant load reflects a higher level of stiffness. Within Shore hardness testing, this attribute is quantified by recording how deeply an indenter penetrates the material's surface, using a durometer equipped with a precision gauge. Materials with greater hardness oppose indentation more effectively, as their internal structure resists the action of the applied force. The relationship between stiffness and hardness was evident, as specimens with higher elastic modulus exhibited greater Shore D hardness. Increasing the dammar content enhanced ductility—reflected by reduced tensile strength and higher elongation at break—thereby lowering stiffness and hardness. The Shore D results

followed the same trend, confirming that higher ductility corresponds to reduced penetration resistance and a softer, more compliant material.

A statistical power analysis confirmed that using 15 specimens per group ensured highly reliable Shore D hardness results (power ≈ 1). No outliers were detected (Dixon test, $\alpha = 0.05$). One-way ANOVA revealed that the dammar content had a very strong effect on hardness ($F = 1524.5$, $p = 7.9\times10^{-81}$). Levene's ($p = 0.48$) and Shapiro–Wilk ($p > 0.05$) tests confirmed homogeneous variances and normal data distribution. Bonferroni post hoc analysis ($\alpha = 0.01$) indicated that all consecutive group pairs showed significant differences ($p < 0.01$). Overall, Shore D hardness decreased progressively with increasing dammar content, confirming reduced stiffness and higher material ductility.

Global Discussion on the Mechanical Behaviour

Based on the combined mechanical and dynamic analyses, the overall behavior of the hybrid composites can be interpreted in terms of polymer network structure and viscoelastic mechanisms. The main effects of increasing dammar content are discussed globally below.

From a polymer physics standpoint, the behavior of the hybrid composites can be explained by the structural and rheological characteristics of the dammar–epoxy matrices. The higher intrinsic viscosity and partially amorphous character of natural dammar, compared with the epoxy component, led to a less densely cross-linked and more heterogeneous polymer network when dammar partially replaced epoxy. Together with the dilution in turpentine, this resulted in a medium-viscosity matrix, comparable in consistency to natural honey, which facilitated adequate wetting of the reinforcement but reduced the overall cross-link density.

The observed decrease in tensile and flexural strength with increasing dammar content can be primarily credited to the reduction in cross-link density and limited chemical compatibility between the dammar and epoxy phases, which weakens interfacial bonding. Dammar, being a natural triterpenoid resin with a partially amorphous structure, restricts epoxy curing and forms a softer, less rigid network, resulting in lower stiffness but greater flexibility.

As the dammar fraction increased, the mobility of polymer chains became more pronounced, leading to a stronger viscoelastic response of the matrix. This enhanced internal mobility promoted higher damping capability and a corresponding decrease in natural frequency, since materials with reduced stiffness and greater internal friction dissipate vibrational energy more effectively. Such trends are consistent with known mechanisms in polymer physics, where reduced cross-link density and increased chain mobility enhance energy dissipation but lower the modulus of elasticity.

Comparison with Similar Studies

The trends observed in this study are consistent with previous reports on chicken feather–based composites. Taghiyari *et al.* (2020) showed that adding chicken feathers to wood–UF panels reduces density and stiffness while maintaining acceptable mechanical performance for light structural applications. Similarly, Kurien *et al.* (2022) and Dutta *et al.* (2024) reported that chicken feather fiber–reinforced composites and biopolymer systems exhibit a clear trade-off between strength and ductility as the bio-based fraction increases. Unlike Kurien *et al.* (2022), the present study extends the topic toward a hybrid dammar–epoxy matrix combined with recovered paper, representing a further step toward fully eco-friendly composites. The present study aligns with such recommendations from

Dutta *et al.* (2024) by developing hybrid dammar–epoxy composites reinforced with both poultry feathers and recovered paper, thereby achieving a better balance between stiffness and ductility while maintaining a high bio-based content. Chandran *et al.* (2024) and Paramasivam *et al.* (2025) also observed that hybrid epoxy or bioepoxy systems containing chicken feathers tend to show decreased tensile and flexural strengths but improved deformability and impact tolerance when the feather or biofiller content is raised. Chandran *et al.* (2024) reported that bioepoxy composites reinforced with waste chicken feather biofillers exhibit good interfacial adhesion but a reduction in mechanical strength at higher filler content. In contrast, the present study employs a hybrid dammar–epoxy matrix combined with both poultry feathers and recovered paper, which enhances structural stability and stiffness while maintaining a high bio-based fraction. Paramasivam *et al.* (2025) demonstrated that hybrid composites reinforced with chicken feathers and Sesbania grandiflora fibers achieved improved strength and thermal stability at an optimal 2:1 fiber ratio. In comparison, the present study replaces the plant fiber with recovered paper and employs a hybrid dammar–epoxy matrix, achieving similar reinforcement synergy through bio-based hybridization and demonstrating the feasibility of eco-friendly composites. The tensile strength obtained in the present study (64 to 78 MPa, Fig. 4) is considerably higher than the one reported by Paramasivam *et al.* (2025) for feather–plant-fiber hybrid composites, confirming the superior load-transfer efficiency of the dammar–epoxy matrix and the reinforcing synergy between poultry feathers and recovered paper.

In terms of novelty, the present work introduces a dual level of hybridization—both in the reinforcement and in the matrix—which has not been previously reported for feather-based composites. Compared with the studies mentioned in the previous paragraph, the present work provides several improvements and complementary insights. First, it combines two waste-derived reinforcements—poultry feathers and recovered paper—at a constant level of 60 wt% in all formulations, allowing the isolated effect of matrix composition (dammar percentage) to be assessed. Second, the hybrid matrix is based on a partially bio-derived resin (dammar), which increases the renewable fraction of the composite without completely sacrificing mechanical performance. Third, the materials were characterized under multiple loading modes (tension, compression, bending, Shore D hardness, and free vibrations), offering a more comprehensive overview of their behavior than studies limited to a single mechanical test. Finally, the use of statistical power analysis, Dixon outlier detection, one-way and Welch ANOVA, Levene and Shapiro–Wilk tests, and Bonferroni post hoc comparisons ensures that the observed trends are not only qualitatively evident but also quantitatively validated. These aspects position the present composites as promising candidates for furniture elements and interior components where a balance between reduced stiffness, enhanced damping, and a high bio-based content is desirable.

Microstructural Characterization

Microstructural analysis was performed on one representative specimen from each material category listed in Table 1. The lateral surface, front surface, and fracture cross-section were examined using an INSIZE stereomicroscope at a magnification of 10×. These observations provided visual information on the structural uniformity, adhesion between layers, and fracture morphology of the hybrid composites. Subsequently, the lateral cross-sections of the specimens were examined in greater detail at 500× magnifications using an OLYMPUS optical microscope. These observations aimed to identify possible pores, material defects, or resin–reinforcement interfacial gaps within the hybrid composite structure.

From a macroscopic standpoint (see Fig. 14), the surface of the hybrid composites appeared uniform and well consolidated. No visible pores, cracks, or manufacturing defects were observed, confirming a good impregnation of the reinforcement and adequate adhesion between the feathers and the matrix.

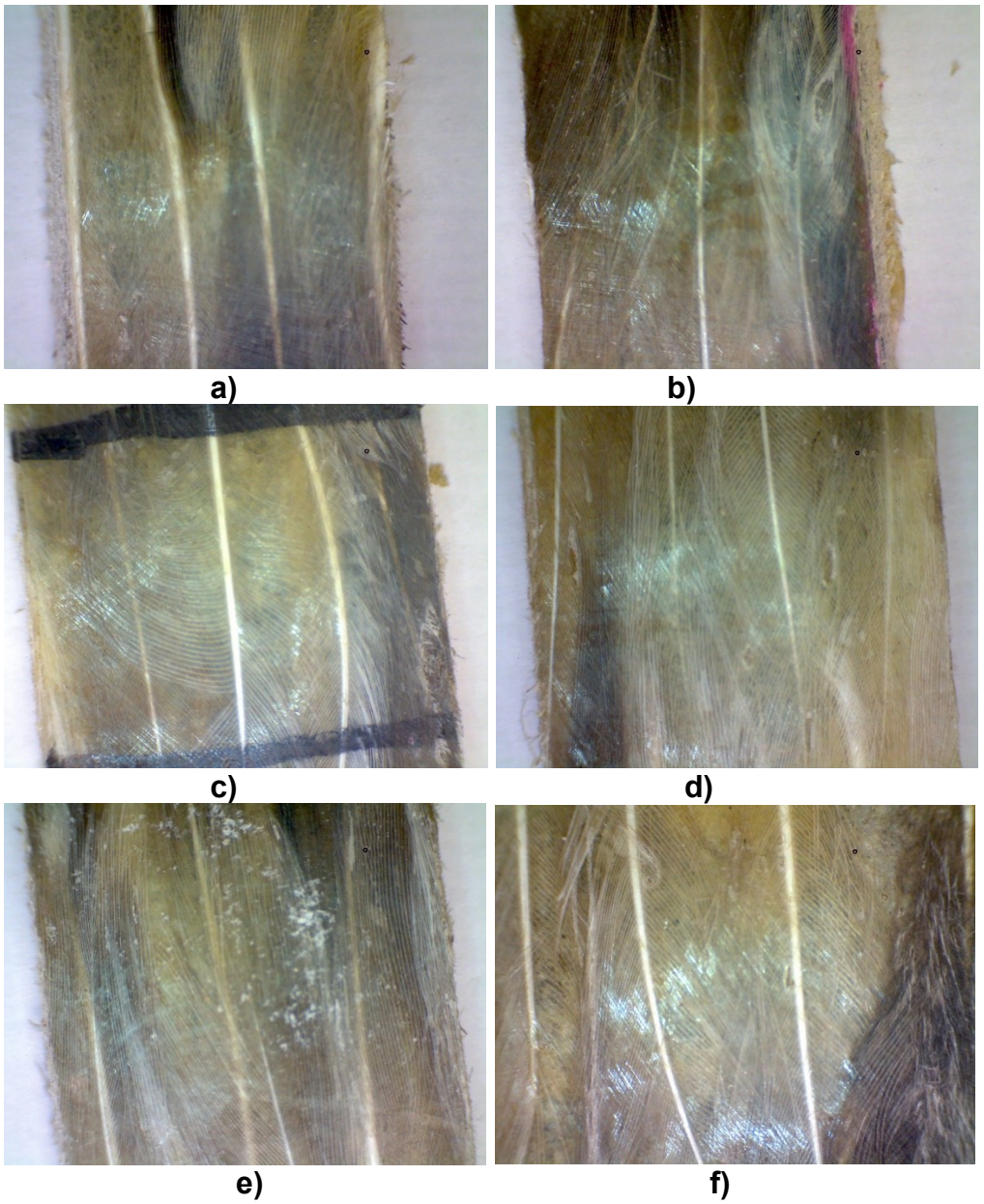

Fig. 14. Macroscopic analysis of one representative specimen from each material set – front view (10x): a) D0, b) D50, c)D55, d) D60, e)D65, f)D70.

The side microstructural analysis (see Fig. 15) revealed a compact, well-bonded layered structure without significant voids or delaminations. The resin was evenly distributed through the laminae, ensuring good adhesion between the paper and feather layers.

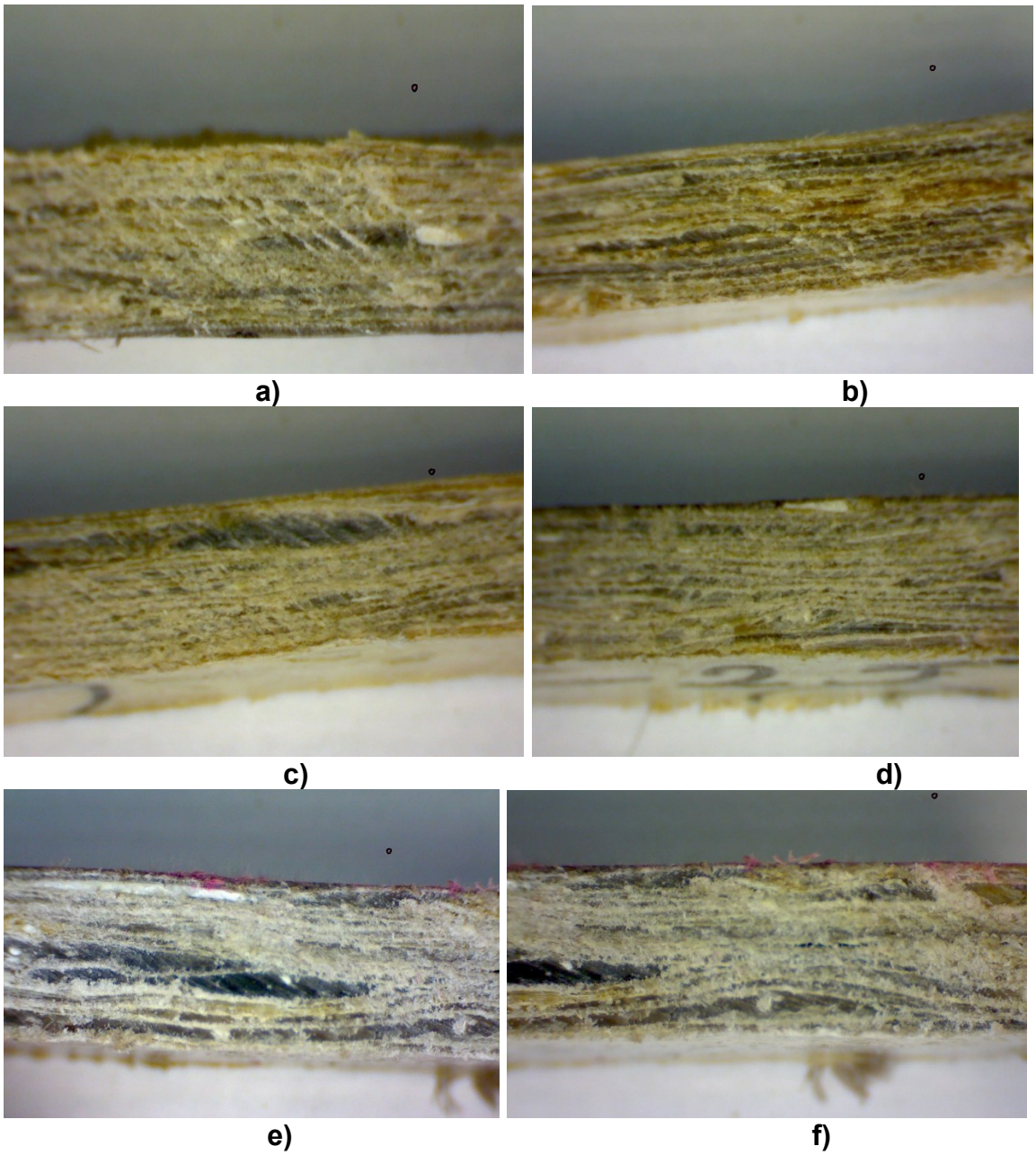

Fig. 15. Macroscopic analysis of one representative specimen from each material set – side view (10x): a) D0, b) D50, c)D55, d) D60, e)D65, f)D70.

Macroscopic examination of the fracture surfaces (see Fig. 16) revealed a compact and cohesive structure with no major delaminations or resin pull-out. The matrix exhibited good impregnation around the feathers, confirming strong adhesion and an efficient load transfer between the reinforcement and the hybrid resin system. It was also observed that as the proportion of dammar in the resin increased, the fracture surface became more irregular compared with the specimens containing only synthetic resin (compare, for example, Fig. 16.a with 16.f), where the fracture occurred abruptly and almost perpendicular to the longitudinal symmetry axis. This behavior is typical of more ductile materials, where increased deformability leads to a rougher and less planar fracture surface.

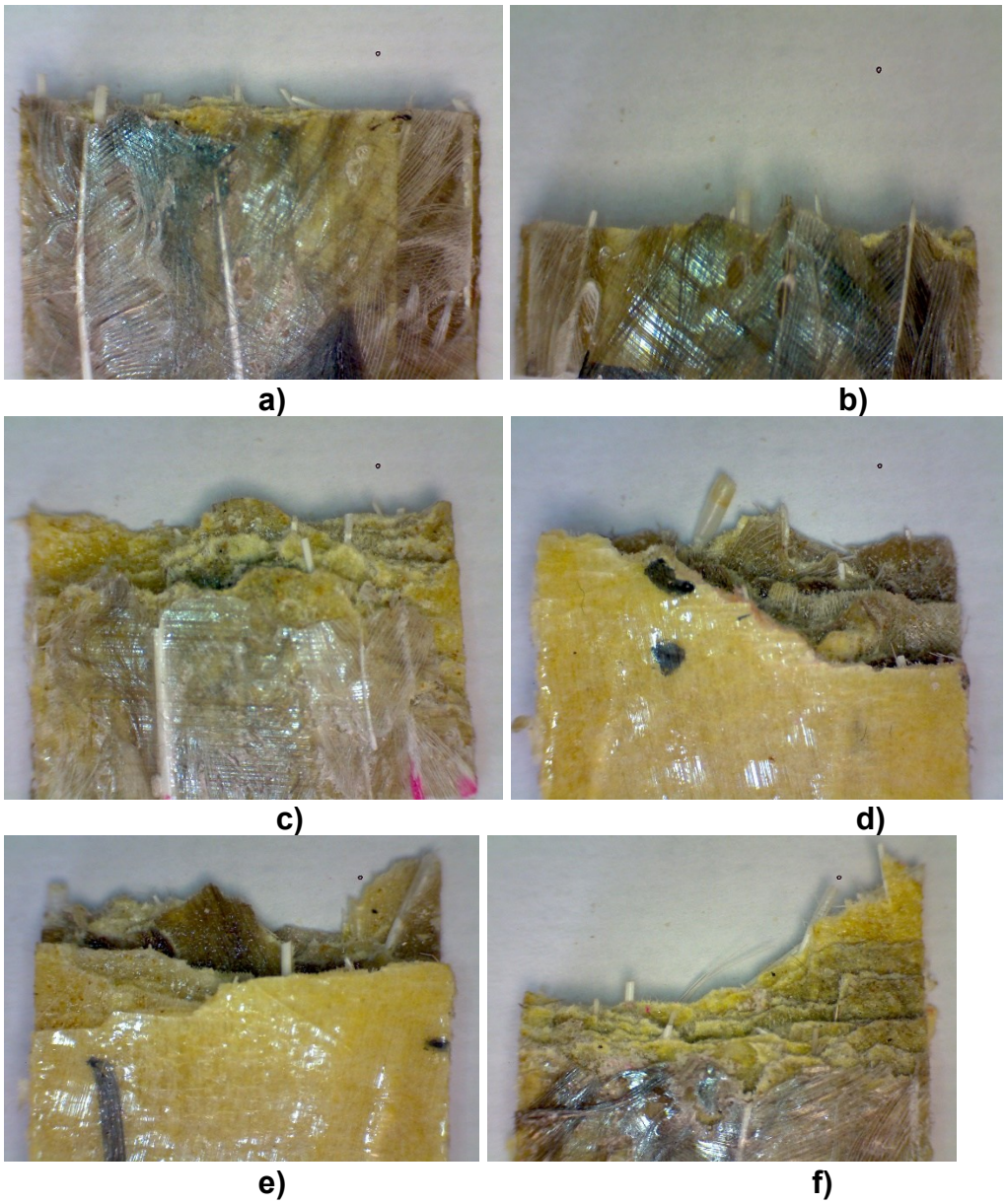

Fig. 16. Macroscopic analysis of one representative specimen from each material set – tensile breaking section (10x): a) D0, b) D50, c)D55, d) D60, e)D65, f)D70

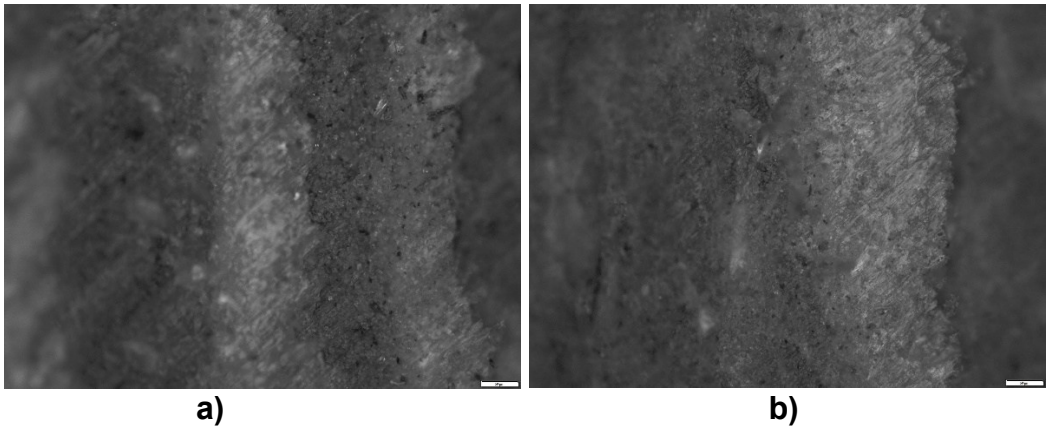

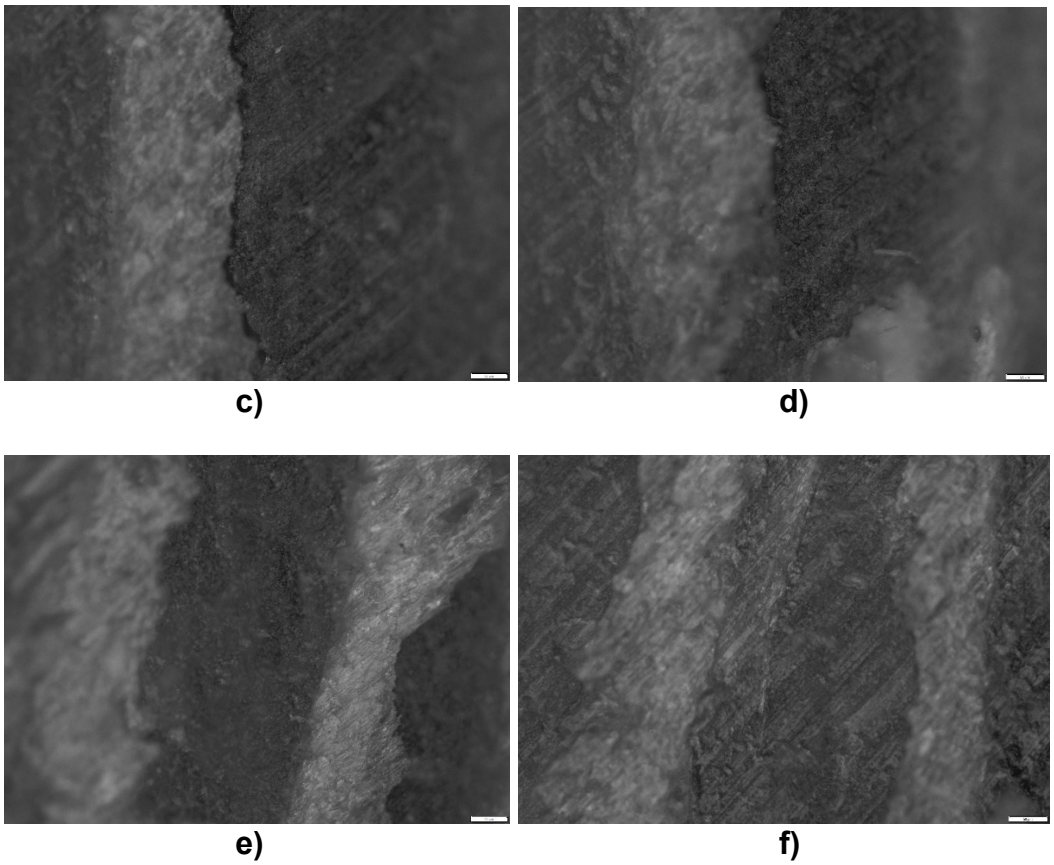

Fig. 17. Microscopic analysis of one representative specimen from each material set – side view (500x): a) D0, b) D50, c)D55, d) D60, e)D65, f)D70

The 500× optical micrographs of the lamina–matrix interface revealed a uniform microstructure, with well-defined boundaries between the lamina and the resin matrix (see Fig. 17). No significant porosity or interfacial detachment was observed, indicating satisfactory resin impregnation. The contact surface between the lamina and the hybrid matrix appeared continuous, suggesting proper adhesion and wetting during curing.

CONCLUSIONS

1. An increase in the proportion of dammar in the hybrid matrix led to a reduction in mechanical strengths (tensile, compressive, and flexural), while specific deformations increased (elongation at break, compressive and flexural displacements).
2. In vibration tests, the natural frequency decreased significantly with higher dammar content, confirming reduced stiffness, whereas the damping factor increases, indicating greater elasticity and improved energy dissipation capacity.
3. For Shore D hardness, the values decreased progressively and significantly with the increase in dammar percentage, confirming reduced stiffness and a tendency toward more ductile behavior.
4. Statistical analyses (power analysis, ANOVA, Levene, Shapiro–Wilk, and post hoc Bonferroni) demonstrated that the results were robust (the power analysis was almost

equal to 1), variances are homogeneous, distributions were close to normal, and the differences between groups were statistically significant in most cases.

5. Incorporating dammar in higher proportions (higher than 55%) led to a stabilization of its effect on bending strength, but the trend of increased deformability (elongation at break or traverse stroke) and damping (from free vibrations) remained evident.
6. The combination of recycled paper and poultry feathers proved to be an effective reinforcement material, providing good compatibility and adhesion to the matrix, confirmed by the mechanical results and the absence of major defects (no defects or areas with voids were observed in the samples side sections).
7. From an application standpoint, these composites showed promise for building furniture parts or interior decorations.
8. The microstructural analysis confirmed that the fabricated composites exhibited good structural cohesion, with well-bonded interfaces and uniform resin distribution, ensuring mechanical stability and reproducibility across all material variants.

REFERENCES CITED

Abdel-Ghani, M., Edwards, H. G. M., Stern, B., and Janaway, R. (2009). "Characterization of paint and varnish on a medieval Coptic-Byzantine icon: Novel usage of dammar resin," *Spectrochimica Acta Part A* 73, 566-575. https://doi.org/10.1016/j.saa.2008.10.050

Alashwal, B. Y., Bala, M. S., Gupta, A., Sharma, S., and Mishra, P. (2020). "Improved properties of keratin-based bioplastic film blended with microcrystalline cellulose: A comparative analysis," *Journal of King Saud University – Science* 32(1), 853-857. https://doi.org/10.1016/j.jksus.2019.03.006

Álvarez-del-Castillo, M. D., Garrido-Soriano, N., Casadesús, M., Macanás, J., Molins-Duran, G., and Carrillo-Navarrete, F. (2022). "Environmental impact of chicken feathers based polypropylene composites developed for automotive and stationary applications and comparison with glass-fibre analogues," *Waste and Biomass Valorization* 13, 4585-4598. https://doi.org/10.1007/s12649-022-01810-0

Amieva, E. J. C., Velasco-Santos, C., Martínez-Hernández, A. L., Rivera-Armenta, J. L., Mendoza-Martínez, A. M., and Castaño, V. M. (2015). "Composites from chicken feather quill and recycled polypropylene," *Journal of Composite Materials* 49(3), 275-283. https://doi.org/10.1177/0021998313518359

ASTM D695 (2016). "Standard test method for compressive properties of rigid plastics," ASTM International, West Conshohocken, PA, USA.

ASTM D790-17 (2017). "Standard test methods for flexural properties of unreinforced and reinforced plastics and electrical insulating materials," ASTM International, West Conshohocken, PA, USA.

ASTM D2240-17 (2021). "Standard test method for rubber property—Durometer hardness," ASTM International, West Conshohocken, PA, USA.

ASTM D3039 (2014). "Standard test method for tensile properties of polymer matrix composite materials," ASTM International, West Conshohocken, PA, USA.

Barone, J. R., and Schmidt, W. F. (2005). "Polyethylene reinforced with keratin fibers obtained from chicken feathers," *Composites Science and Technology* 65(2), 173-181. https://doi.org/10.1016/j.compscitech.2004.06.011

BKSV (2025). "Piezoelectric Charge Accelerometer Type 8309," (https://www.bksv.com/-/media/literature/Product-Data/bp2053.ashx?), Accessed November 11, 2025

Bolcu, D., Stănescu, M. M., Mirițoiu, C. M., Ciucă, I., Bolcu, A., and Rădoi, I. A. (2024). "The influence of hybrid matrices based on dammar on the mechanical properties of composites with chopped corn cobs reinforcement," *Materiale Plastice* 61(3), 27-38. https://doi.org/10.37358/MP.24.3.5730

Bonaduce, I., Odlyha, M., Di Girolamo, F., Lopez-Aparicio, S., Grøntoft, T., and Colombini, M. P. (2013). "The role of organic and inorganic indoor pollutants in museum environments in the degradation of dammar varnish," *Analyst* 138, 487-500. https://doi.org/10.1039/c2an36259g

Brandelli, A. (2008). "Bacterial keratinases: Useful enzymes for bioprocessing agroindustrial wastes and beyond," *Food and Bioprocess Technology* 1(2), 105-116. https://doi.org/10.1007/s11947-007-0025-y

Caovilla, M., Demaman Oro, C. E., Mores, R., Venquiaruto, L. D., Mignoni, M. L., Di Luccio, M., Treichel, H., Dallago, R. M., and Tres, M. V. (2025). "Exploring chicken feathers as a cost-effective adsorbent for aqueous dye removal," *Separations* 12(2), 39. https://doi.org/10.3390/separations12020039

Chandran, A. J., Rangappa, S. M., Suyambulingam, I., and Siengchin, S. (2024). "Waste chicken feather biofiller reinforced bioepoxy resin-based biocomposites – A waste-to-wealth experimental approach," *International Journal of Biological Macromolecules* 261(Part 1), article 129708. https://doi.org/10.1016/j.ijbiomac.2024.129708

Cheng, S., Lau, K. T., Liu, T., Zhao, Y., Lam, P.-M., and Yin, Y. (2009). "Mechanical and thermal properties of chicken feather fiber/PLA green composites," *Composites Part B: Engineering* 40(7), 650-654. https://doi.org/10.1016/j.compositesb.2009.04.011

Clearfield, A. (2000). "Inorganic ion exchangers, past, present and future," *Solvent Extraction and Ion Exchange* 18(4), 655-678. https://doi.org/10.1080/07366290008934702

Cioffi, M. G. A., de Oliveira, D. M., de Bomfim, A. S. C., de Carvalho Benini, K. C. C., Cioffi, M. O. H., and Voorwald, H. J. C. (2022). "Thermo-mechanical properties of polypropylene composites filled with recycled office waste paper," *Journal of Thermoplastic Composite Materials* 19(16), 14089-14101. https://doi.org/10.1080/15440478.2022.2116517

Ciucă, I., Stănescu, M. M., Bolcu, D., Mirițoiu, C. M., and Rădoi, A. I. (2022). "Study of mechanical properties for composite materials with hybrid matrix based on dammar and natural reinforcers," *Environ. Eng. Manag. J.* 21, 299-307.

Dieckmann, E., Onsiong, R., Nagy, B., Sheldrick, L., Cheeseman, C. (2021). "Valorization of waste feathers in the production of new thermal insulation materials," *Waste and Biomass Valorization* 12, 1119-1131. https://doi.org/10.1007/s12649-020-01007-3

Dutta, H., Bora, D., Chetia, P., Bharadwaj, C., Purbey, R., Bohra, R. C., Dutta, K., Rajulu, A. V., Sadiku, E. R., Selvam, S. P., Gurusamy, P., Rawal, R. K., and Jayaramudu, J. (2024). "Biopolymer composites with waste chicken feather fillers: A review," *Renewable and Sustainable Energy Reviews* 197, article 114394. https://doi.org/10.1016/j.rser.2024.114394

Engin, M., and Konukçu, A. Ç. (2024). "Physical and mechanical properties of fiberboard produced with shredded waste office paper," *BioResources* 19(4), 8642–8653. https://doi.org/10.15376/biores.19.4.8642-8653

European Commission (2023). "Biomass," (https://energy.ec.europa.eu/topics/renewable-energy/bioenergy/biomass_en), Accessed July 29, 2025.

Foita de Aur (2023). "Foita de aur. Magazin materiale de pictura," (https://foitadeaurmagazin.ro/), Accessed September 23, 2023.

Franz, M. H., Neda, I., Maftei, C. V., Ciucă, I., Bolcu, D., and Stănescu, M. M. (2021). "Studies of chemical and mechanical properties of hybrid composites based on natural resin dammar formulated by epoxy resin," *Polym. Bul.* 78, 2427-2438. https://doi.org/10.1007/s00289-020-03221-4

Ghodake, G., Shinde, S., Saratale, G. D., Kadam, A., Saratale, R. G., and Kim, D.-Y. (2020). "Water purification filter prepared by layer-by-layer assembly of paper filter and polypropylene-polyethylene woven fabrics decorated with silver nanoparticles," *Fibers and Polymers* 21, 751-761. https://doi.org/10.1007/s12221-020-9624-2

Gunawan, G., Heryanto, H., and Tahir, D. (2024). "Keratin-based bioplastics extracted from chicken feathers: Effect of chitosan concentration on the structural, chemical bonding, and mechanical properties of bioplastics," *International Journal of Biological Macromolecules* 265(Part 1), article 130722. https://doi.org/10.1016/j.ijbiomac.2024.130722

Hurtado, P. L., Rouilly, A., Vandenbossche, V., and Raynaud, C. (2016). "A review on the properties of cellulose fibre insulation," *Building and Environment* 96, 170-177. https://doi.org/10.1016/j.buildenv.2015.09.031

IQ Economy+ (2024). "Hartie copiator A3 IQ Economy+ 80 g/mp 500 coli/top," (https://www.bnb.ro/hartie-copiator-a3-iq-economy-80-g-mp-500-coli-top.html), Accessed February 5, 2024.

Juarros-Basterretxea, J., Aonso-Diego, G., Postigo, Á., Montes-Álvarez, P., Menéndez Aller, Á., and García-Cueto, E. (2024). "Post-hoc tests in one-way ANOVA: The case for normal distribution," *Methodology: European Journal of Research Methods for the Behavioral and Social Sciences* 20(2), 84-99. https://doi.org/10.5964/meth.11721

Kiew, K. S., Hamdan, S., and Rahman, M. R. (2013). "Comparative study of dielectric properties of chicken feather/kenaf fiber reinforced unsaturated polyester composites," *BioResources* 8(2), 1591-1603. https://doi.org/10.15376/biores.8.2.1591-1603

Kremer Pigmente. (2024). "79300 – 79330 Dammar Varnish," (https://www.kremer-pigmente.com/), Accessed October 14 2024

Kurien, R. A., Biju, A., Raj, K. A., Chacko, A., Joseph, B., and Koshy, C. P. (2022). "Chicken feather fiber reinforced composites for sustainable applications," *Materials Today: Proceedings* 58(3), 862-866. https://doi.org/10.1016/j.matpr.2021.10.400

La Nasa, J., Degano, I., Modugno, F., and Colombini, M. P. (2014). "Effects of acetic acid vapour on the ageing of alkyd paint layers: Multi-analytical approach for the evaluation of the degradation processes," *Polymer Degradation and Stability* 105, 257-264. https://doi.org/10.1016/j.polymdegradstab.2014.04.010

Marín-Calvo, N., González-Serrud, S., and James-Rivas, A. (2023). "Thermal insulation material produced from recycled materials for building applications: Cellulose and rice husk-based material," *Frontiers in Built Environment* 9, article 1271317. https://doi.org/10.3389/fbuil.2023.1271317

Maurya, S. D., and Singh, A. (2023). "Application and future perspectives of keratin protein extracted from waste chicken feather: A review," *Sustainable Chemical Engineering* 5(1), 31-45. https://doi.org/10.37256/sce.5120243521

Mirițoiu, C. M., Stănescu, M. M., and Bolcu, D. (2020). "Research regarding the mechanical properties of a new hybrid vegetal resin," *Mater. Plast.* 57, 37-45. https://doi.org/10.37358/Mat.Plast.1964

Miritoiu, C. M. (2024). "Influence of dammar resin on the mechanical properties of composites reinforced with corn husk and paper waste," *BioResources* 19(4), 9416-9446. https://doi.org/10.15376/biores.19.4.9416-9446

Miriţoiu, C. M. (2025). *Scientific Research by Analysis and Design of Experiments*, SITECH Publishing House, Craiova, Romania.

Mittal, H., Kaith, B. S., and Jindal, R. (2010). "Synthesis, characterization and swelling behaviour of poly (acrylamide-co-methacrylic acid) grafted gum ghatti based superabsorbent hydrogels," *Advances in Applied Science Research* 1(3), 56-66.

Mokrejš, P., Huťťa, M., Pavlackova, J., Egner, P. (2017). "Preparation of keratin hydrolysate from chicken feathers and its application in cosmetics," *Journal of Visualized Experiments* 2017(129), article e56254. https://doi.org/10.3791/

Mrajji, O., El Wazna, M., Boussoualem, Y., El Bouari, A., and Cherkaoui, O. (2021). "Feather waste as a thermal insulation solution: Treatment, elaboration and characterization," *J. Ind. Text.* 50, 1674-1697. https://doi.org/10.1177/1528083719869393

Okoya, A. A., Ochor, N. O., Akinyele, A. B., and Olaiya, O. E. (2020). "The use of chicken feather waste as an adsorbent for crude oil clean-up from polluted water," *Journal of Agriculture and Ecology Research International* 21(3), 30-36. https://doi.org/10.9734/jaeri/2020/v21i330136

Oluba, O. M., Obi, C. F., Akpor, O. B., Ojeaburu, S. I., Ogunrotimi, F. D., Adediran, A. A., and Oki, M. (2021). "Fabrication and characterization of keratin–starch biocomposite film from chicken feather waste and ginger starch," *Scientific Reports* 11, article 8768. https://doi.org/10.1038/s41598-021-88002-3

Ossai, I. C., Hamid, F. S., Hassan, A. (2022). "Valorisation of keratinous wastes: A sustainable approach towards a circular economy," *Waste Manag.* 151, 81-104. https://doi.org/10.1016/j.wasman.2022.07.021

Ott, R. L., and Longnecker, M. (2021). *Introduction to Statistical Methods and Data Analysis*, Cengage Learning Publisher, Boston, MA, USA.

Paramasivam, S. K., Marimuthu, M., Sakthivel, A., Rajasekar, J., Palanisamy, S., Mausam, K., and Al-Farraj, S. A. (2025). "Mechanical and thermal behavior analysis of chicken feather/*Sesbania grandiflora* fibers-based hybrid epoxy composites," *BioResources* 20(4), 8591-8610. https://doi.org/10.15376/biores.20.4.8591-8610

Park, S. K., Bae, D., and Hettiarachchy, N. (2000). "Protein concentrate and adhesives from meat and bone meal," *J. Am. Oil Chem. Soc.* 77(11), 1223-1227. https://doi.org/10.1007/s11746-000-0191-5

Petcu, C., Hegyi, A., Stoian, V., Dragomir, C. S., Ciobanu, A. A., Lăzărescu, A.-V., and Florean, C. (2023). "Research on thermal insulation performance and impact on indoor air quality of cellulose-based thermal insulation materials," *Materials (Basel)* 16(15), article 5458. https://doi.org/10.3390/ma16155458

Polydis. (2023). "Polydis," (https://polydis.ro/), Accessed September 7, 2023.

Popescu, D. A., Tuculina, M. J., Diaconu, O. A., Gheorghit, L. M., Nicolicescu, C., Cumpătă, C. N., Petcu, C., Abdul-Razzak, J., Rîcă, A. M., and Voinea-Georgescu, R. (2023) "Effects of dental bleaching agents on the surface roughness of dental restoration materials," *Medicina* 59, 1-18. https://doi.org/10.3390/medicina59061067

Prambauer, M., Paulik, C., and Burgstaller, C. (2015). "Mechanical properties of structural paper-polypropylene composite laminates," *Materials Science Forum* 825-826, 11-18. https://doi.org/10.4028/www.scientific.net/MSF.825-826.11

Puri, V. P., and Jatkar, D. D. (1974). "Use of phenolic resins for conversion of paper to oil filters," *IPPTA* 11(4), 317-319.

Rajabi, M., Ali, M., McConnell, M., and Cabral, J. (2020). "Keratinous materials: Structures and functions in biomedical applications," *Mater. Sci. Eng. C* 110, article 110612. https://doi.org/10.1016/j.msec.2019.110612

Ramakrishnan, N., Sharma, S., Gupta, A., and Alashwal, B. Y. (2018). "Keratin-based bioplastic film from chicken feathers and its characterization," *International Journal of Biological Macromolecules* 111, 352-358. https://doi.org/10.1016/j.ijbiomac.2018.01.037

Real Statistics. (2025). "Real statistics using excel," (https://real-statistics.com/statistics-tables/shapiro-wilk-table/), Accessed August 14, 2025.

Resoltech. (2025). "Resoltech 1050 structural lamination epoxy system," (https://www.resoltech.com/en/markets/1050-detail.html), accessed November 11, 2025

Science Daily (2009). "Need hydrogen storage? Think poultry," (https://www.science.org/content/article/need-hydrogen-storage-think-poultry), Accessed August 13, 2025.

Shapiro, S. S., and Wilk, M. B. (1965). "An analysis of variance test for normality (complete samples)," *Biometrika* 52, 591-611. https://doi.org/10.2307/2333709

Škerget, M., Čolnik, M., Fras Zemljič, L., Gradišnik, L., Živković Semren, T., Tariba Lovaković, B., and Maver, U. (2023). "Efficient and green isolation of keratin from poultry feathers by subcritical water," *Polymers* 15(12), article 2658. https://doi.org/10.3390/polym15122658

Solís-Moreno, C. A., Cervantes-González, E., and Saavedra-Leos, M. Z. (2021). "Use and treatment of chicken feathers as a natural adsorbent for the removal of copper in aqueous solution," *Journal of Environmental Health Science and Engineering* 19(1), 707-720. https://doi.org/10.1007/s40201-021-00639-4

Soon, W. L., Peydayesh, M., de Wild, T., Donat, F., Saran, R., Müller, C. R., Gubler, L., Mezzenga, R., and Miserez, A. (2023). "Renewable energy from livestock waste valorization: Amyloid-based feather keratin fuel cells," *ACS Applied Materials & Interfaces* 15(40), 48458-48467. https://doi.org/10.1021/acsami.3c10218

Stanimir, A., and Pascu, I. (2014). *Design of Experiments with Applications in Manufacturing of Mechanical Products*, Genessa Publishing House, Craiova, Romania.

Statistics Kingdom (2025). "Statistics online," (https://www.statskingdom.com/index.html), Accessed August 14, 2025.

Stănescu, M. M. (2015). "A study regarding the mechanical behaviour of Dammar based composite materials, reinforced with natural fiber fabrics," *Mater. Plast.* 52, 596-600.

Stevulova, N., Hospodarova, V., and Junak, J. (2016). "Potential utilization of recycled waste paper fibres in cement composites," *Cheminė Technologija* 67(1), 55-61. https://doi.org/10.5755/j01.ct.67.1.15001

Taghiyari, H. R., Majidi, R., Esmailpour, A., Sarvari Samadi, Y., Jahangiri, A., and Papadopoulos, A. N. (2020). "Engineering composites made from wood and chicken feather bonded with UF resin fortified with wollastonite: A novel approach," *Polymers* 12(4), article 857. https://doi.org/10.3390/polym12040857

Tesfaye, T., Sithole, B., and Ramjugernath, D. (2017). "Valorisation of chicken feathers: A review on recycling and recovery route—Current status and future prospects," *Clean Technol. Environ. Policy* 19, 2363-2378. https://doi.org/10.1007/s10098-017-1443-9

Tesfaye, T., Sithole, B., Ramjugernath, D., and Chunilall, V. (2017). "Valorisation of chicken feathers: Characterisation of chemical properties," *Waste Management* 68(9), 626-635.

Topp, N. E., and Pepper, K. W. (1949). "Properties of ion-exchange resins in relation to their structure, Part I. Titration curves," *Journal of the Chemical Society* 690, 3299-3303.

Trojanowska, D. J. (2023). "Preparation of new keratin-based bioplastics," PhD Thesis, Department of Materials Science, University of Milano-Bicocca, Italy. https://boa.unimib.it/handle/10281/417305

Ukkola, J., Lampimäki, M., Laitinen, O., Vainio, T., Kangasluoma, J., Siivola, E., Petäjä, T., and Liimatainen, H. (2021). "High-performance and sustainable aerosol filters based on hierarchical and crosslinked nanofoams of cellulose nanofibers," *Journal of Cleaner Production* 296, article 127498. https://doi.org/10.1016/j.jclepro.2021.127498

UNLOCK Project (2025). "From poultry waste to packaging: The feather-based bioplastic," (https://www.packnode.org/en/sustainability/from-poultry-waste-to-packaging-the-feather-based-bioplastic), Accessed August 13, 2025.

Veerabadran, V., Balasundari, S. N., Devi, D. M., and Kumar, D. M. (2012). "Optimisation and production of proteinacious chicken feather fertiliser by proteolytic activity of *Bacillus* sp. MPTK 6," *Indian J. Innov. Dev.* 1(3), 193-198.

Villa, A. L. V., Aragão, M. R. S., dos Santos, E. P., Mazotto, A. M., Zingali, R. B., de Souza, E. P., and Vermelho, A. B. (2013). "Feather keratin hydrolysates obtained from microbial keratinases: effect on hair fiber," *BMC Biotechnology* 13, 15. https://doi.org/10.1186/1472-6750-13-15

Wang, Z., Li, H., Jiang, Z., and Chen, Q. (2018). "Effect of waste paper fiber on properties of cement-based mortar and relative mechanism," *Journal of Wuhan University of Technology - Materials Science Edition* 33, 419-426.

Wang, Z., and Wang, D. (2023). "Can paper waste be utilised as an insulation material in response to the current crisis," *Sustainability* 15(22), article 15939. https://doi.org/10.3390/su152215939

Zahara, I., Arshad, M., Naeth, M. A., Siddique, T., and Ullah, A. (2021). "Feather keratin derived sorbents for the treatment of wastewater produced during energy generation processes," *Chemosphere* 273, article 128545. https://doi.org/10.1016/j.chemosphere.2020.128545

Zar, J. H. (1999). *Biostatistical Analysis* (5th Ed.), Pearson Prentice Hall, Hoboken, NJ, USA.

Zhang, X., and Wang, R. (2012). "Study on structure and mechanical properties of recycled polypropylene/old paper fiber composites," *China Plastics* 26(4), 102-105. https://doi.org/10.19491/j.issn.1001-9278.2012.04.020

Zubair, M., Roopesh, M. S., and Ullah, A. (2022). "Nano-modified feather keratin derived green and sustainable biosorbents for the remediation of heavy metals from synthetic wastewater," *Chemosphere* 308(Part 3), article 136339. https://doi.org/10.1016/j.chemosphere.2022.136339

Article submitted: September 2, 2025; Peer review completed: November 22, 2025; Revised version received: November 25, 2025; Accepted: November 30, 2025; Published: December 9, 2025.
DOI: 10.15376/biores.21.1.808-838